6 Ma Age of carving Westernmost Grand Canyon: Reconciling geologic data with combined AFT, (U-Th)/He, and $^{4}He/^{3}He$ thermochronologic data

*Winn[1], Carmen, *Karlstrom[1], Karl E.; Shuster[2, 3], David L.; Kelley[4], Shari; Fox[2, 3, 5], Matthew

[1] Department of Earth and Planetary Science, University of New Mexico, Albuquerque, NM, USA

[2] Department of Earth and Planetary Science, University of California, Berkeley, CA, USA

[3] Berkeley Geochronology Center, 2455 Ridge Road, Berkeley, CA, USA

[4] New Mexico Bureau of Geology and Mineral Resources, New Mexico Institute of Mining and Technology, Socorro, NM, USA

[5] Department of Earth Sciences, University College London, Gower Street, London WC1E 6BT, United Kingdom

*Corresponding authors: cwinn264@unm.edu; kek1@unm.edu

Abstract

Conflicting hypotheses about the timing of carving of the Grand Canyon involve either a 70 Ma ("old") or < 6 Ma ("young") Grand Canyon. This paper evaluates the controversial westernmost segment of the Grand Canyon where the following lines of published evidence firmly favor a "young" Canyon. 1) North-derived Paleocene Hindu Fanglomerate was deposited across the present track of the westernmost Grand Canyon, which therefore was not present at ~55 Ma. 2) The 19 Ma Separation Point basalt is stranded between high relief side canyons feeding the main stem of the Colorado River and was emplaced before these tributaries and the main canyon were incised. 3) Geomorphic constraints indicate that relief generation in tributaries

and on plateaus adjacent to the westernmost Grand Canyon took place after 17 Ma. 4) The late Miocene-Pliocene Muddy Creek Formation constraint shows that no river carrying far-traveled materials exited at the mouth of the Grand Canyon until after 6 Ma.

Interpretations of previously-published low-temperature thermochronologic data conflict with these lines of evidence, but are reconciled in this paper via the integration of three methods of analyses on the same sample: apatite (U-Th)/He ages (AHe), $^{4}He/^{3}He$ thermochronometry ($^{4}He/^{3}He$), and apatite fission-track ages and lengths (AFT). "HeFTy" software was used to generate time-temperature (t-T) paths that predict all new and published $^{4}He/^{3}He$, AH, and AFT data to within assumed uncertainties. These t-T paths show cooling from ~ 100 ℃ to 40-60 ℃ in the Laramide (70-50 Ma), long-term residence at 40-60 ℃ in the mid-Tertiary (50-10 Ma), and cooling to near-surface temperatures after 10 Ma, and thus support a "young" westernmost Grand Canyon.

A subset of AHe data, when interpreted alone (i.e., without $^{4}He/^{3}He$ or AFT data), are better predicted by t-T paths that cool to surface temperatures during the Laramide, consistent with an "old" Canyon. This inconsistency, which mimics the overall controversy, is reconciled by optimizing cooling paths so they are most consistent with multiple thermochronometers from the same rocks and adjusting parameters to account for model uncertainties. We adjusted model parameters to account for uncertainty in the rate of radiation damage annealing during sedimentary burial in these apatites and thus possible changes in He retentivity. In the westernmost Grand Canyon, peak burial conditions (temperature and duration) during the Laramide were likely insufficient to fully anneal radiation damage that accumulated during prolonged, near-surface residence since the Proterozoic. The combined AFT, AHe, and $^{4}He/^{3}He$ analysis of a key sample from Separation Canyon can only be reconciled by a 'young' Canyon,

48 but thermochronologic uncertainties remain large for this geologic scenario. Additional new AFT
49 (5 samples) and AHe (3 samples) data in several locations along the canyon corridor also support
50 a "young" Canyon and suggest the possibility of variable mid-Tertiary thermal histories beneath
51 north-retreating cliffs. We conclude that application of multiple thermochronometers from
52 common rocks reconciles conflicting thermochronologic interpretations and is best explained by
53 a "young" westernmost Grand Canyon.

54 ***Keywords***: Grand Canyon, apatite, thermochronology, (U-Th)/He, fission track, $^{4}He/^{3}He$

55

56 **1. Introduction to the "age of Grand Canyon" controversy**

57 The 140-year-long controversy about the age of the Grand Canyon was initially posed in
58 terms of the hypothesis that the Colorado River was older than the tectonic uplifts it carves
59 across (Powell, 1875; Dutton, 1882) and an alternate hypothesis that a younger river became
60 erosionally superimposed on older, deeper monoclinal structures (Davis, 1901). It has long been
61 recognized that Laramide-aged deposits from north-flowing rivers were present in the
62 westernmost Grand Canyon (Young, 1966; Elston and Young, 1991) and some workers have
63 related these deposits to an "old", Laramide-aged (~70 Ma) Grand Canyon (e.g. Wernicke,
64 2011). As more research in the area was done, early proponents of a "young" (< 6 Ma) Grand
65 Canyon (e.g. Babenroth and Strahler, 1945; Blackwelder, 1934; Longwell, 1946; Lucchitta,
66 1966, 1972; McKee et al., 1967; Strahler, 1948) based their conclusions on the locally-derived
67 Miocene-Pliocene Muddy Creek Fm., which stipulates that no far-traveled material reached the
68 Grand Wash trough through the mouth of the Grand Canyon between ~13 and 6 Ma.

69 Low-temperature apatite thermochronology methods began to be applied to Grand
70 Canyon incision by Naeser et al. (1989) and Kelley et al. (2001). Subsequent studies have

included apatite fission track (AFT), (U-Th)/He ages (AHe), and $^{4}He/^{3}He$ thermochronometry ($^{4}He/^{3}He$) such that the combined data should resolve continuous t-T paths from ~110 °C to surface temperatures of 10-25 °C. AFT relies on the temperature sensitivity of annealing the damage done by spontaneous fission of ^{238}U to the crystal structure. An AFT age is determined by the number of these 'fission tracks' relative to the parent isotope, while the lengths of the tracks (i.e., the degree of shortening from a ~17 µm initial length) provides information about residence time in the partial annealing zone (110-60 °C; Ketcham et al., 2007). AHe dating is sensitive to temperatures of 90-30 °C, where apatite crystals begin retaining radiogenic ^{4}He at different temperatures depending on initial U and Th parent concentrations (Shuster et al., 2006; Flowers, 2009). $^{4}He/^{3}He$ thermochronometry provides additional information about a given sample's continuous cooling path and is especially sensitive to the lowest resolvable temperatures of the three methods (Shuster and Farley, 2005). The datasets, individually and combined, can be used to constrain multiple time-temperature (t-T) cooling paths that predict the data within acceptable statistical confidence. Cooling paths are then related to burial depths by assuming values for surface temperature and geothermal gradient, which in this area are commonly assumed to be 10-25 °C surface temperatures and a 25 °C/km geothermal gradient (Wernicke, 2011; Karlstrom et al., 2014).

Wernicke (2011) hypothesized that a NE-flowing 70-80 Ma California River and then a SW-flowing 55-30 Ma Arizona River both followed the modern Colorado River's current path through the Grand Canyon and carved the canyon to within a few hundred meters of its modern depth by ~50 Ma. In this hypothesis, the Colorado River "was not an important factor in the excavation of Grand Canyon". Flowers and Farley (2012) noted a major difference between eastern and western Grand Canyon cooling histories but supported an "old" westernmost Grand

Canyon and stated: "The western Grand Canyon $^{4}He/^{3}He$ and AHe data demand a substantial cooling event at 70-80 Ma, and provide no evidence for the strong post-6 Ma cooling signal predicted by the young canyon model." Flowers and Farley (2013) further supported the conclusion of "... apatite $^{4}He/^{3}He$ and (U-Th)/He (AHe) evidence for carving of the western Grand Canyon to within a few hundred meters of modern depths by ~70 million years ago (Ma)".

Other workers have proposed a more complex landscape evolution for individual canyon segments (Figure 1A, inset map). Laramide rivers flowed generally north across the Grand Canyon-Colorado Plateau region (McKee et al., 1967; Young, 2001), perhaps following the Hurricane fault system (Figure 1; Karlstrom et al., 2014). Thermal histories generated by AHe and AFT data from Lee et al. (2013) and Karlstrom et al. (2014) indicated different cooling histories for rim and river-level rocks in the Eastern Grand Canyon before 25 Ma but similar temperatures after 15 Ma, indicating that no canyon existed in this segment until the incision of an East Kaibab paleocanyon at 25-15 Ma. Thermochronologic data from these studies and others (Warneke, 2015) also indicate that Marble Canyon was not incised until the past 5-6 Ma.

Karlstrom et al. (2014) proposed a "paleocanyon solution" whereby an "old" 70-55 Ma paleocanyon segment paralleling the Hurricane fault and an "intermediate" NW-flowing 25-15 Ma East Kaibab paleocanyon segment got linked together by the 5-6 Ma Colorado River as it was downwardly integrated from the Colorado Plateau to the Gulf of California. In this hypothesis, most of the Grand Canyon was incised by the Colorado River in the past 6 Ma. Karlstrom et al. (2016) reinforced this paleocanyon hypothesis and suggested that the 25-15 Ma East Kaibab paleocanyon was carved by an ancestral Little Colorado (not Colorado) River. Laramide (70-50 Ma) thermochronologic ages seen in many samples of that study were

attributed to northward cliff retreat of Mesozoic strata off the Mogollon highlands rather than carving of a ~70 Ma Grand Canyon. Fox and Shuster (2014) proposed that thermochronologic data from the westernmost Grand Canyon were compatible with "young" incision provided that sufficient radiation damage was retained during burial, thereby effectively changing the predicted temperature sensitivity of the system at the time of canyon incision. However, interpretations of thermochronology data from the westernmost Grand Canyon segment remain in controversy (Flowers et al., 2015).

Here we applied the three different thermochronology methods using apatite from the same sample from the westernmost Grand Canyon to resolve conflicting thermal histories generated by inverse modeling of data originating from the same sample. Our key sample (sample #1; see Table 1) has new, high precision $^{4}He/^{3}He$ data, multiple AHe ages, and AFT data and is from the same location as the single Flowers and Farley (2012) $^{4}He/^{3}He$ sample (#2) upon which their "old" Canyon conclusion was mainly based. These are from Separation Canyon, RM 240, where RM = river miles downstream of Lees Ferry (Stevens, 1983). We also report two new samples with combined AFT and AHe data and two new samples with AFT data that span from RM 225-260. Our objective is to re-evaluate and reconcile all new and published thermochronologic data from the westernmost Grand Canyon including AFT and AHe from Lee et al. (2013), AHe from Flowers et al. (2008), and $^{4}He/^{3}He$ from Flowers and Farley (2012).

Westernmost Grand Canyon is defined as the segment between Diamond Creek (RM 225) and the Grand Wash Cliffs (RM 276) (Figure 1). We use the term "old" Canyon for time-temperature (t-T) paths that have a single cooling pulse at 70-55 Ma during which rocks cool to <30 °C and hence to within ~200 m of river level using a 25 °C surface temperature and a 25 °C/km geothermal gradient (Wernicke, 2011). We use the term "young" Canyon for either a

single-stage cooling history that does not reach temperatures of <30 °C or a two-stage cooling history with cooling pulses at 70-50 Ma and at < 6 Ma separated by a period of long-term residence at temperatures of 40-60 °C. These temperatures correspond to burial by 0.8 to 1.4 km of sedimentary rock, the depth of the modern westernmost Grand Canyon measured from the south and north rims respectively, and indicate no westernmost Grand Canyon had been carved.

2. Summary of recent geologic studies supporting a < 6 ma westernmost Grand Canyon

Several recent studies have reinforced the evidence for a "young" 5-6 Ma westernmost Grand Canyon, independent of thermochronology-based studies. "Rim gravels" (e.g. Young, 2001) on the Hualapai Plateau (Figure 1A) document an aggrading base level from 65-55 Ma (Music Mountain Formation), through ~24 Ma (Buck and Doe Formation), to younger than ~19 Ma (Coyote Springs Formation), aggradation which is incompatible with a deep paleocanyon of near-modern depth during this time (Young and Crow, 2014). The Paleocene Music Mountain Formation is interbedded with the Hindu Fanglomerate (see star in Figure 1A and 1C), which locally contains clasts sourced from the Kaibab escarpment to the north and precludes the presence of a paleo-Grand Canyon in the Eocene (Young and Crow, 2014). The 19 Ma Separation Point basalt (Wenrich et al., 1995) overlies the Buck and Doe Formation in a location on the Hualapai Plateau that has been steeply incised on all sides (Figure 1B) suggesting lowering of base level after 19 Ma (Young and Crow, 2014).

Darling and Whipple (2015) examined the longitudinal profiles of Colorado River tributary drainages and compared them to profiles of similar-sized drainages established on the 17 Ma Grand Wash escarpment. From this comparison, Darling and Whipple (2015) concluded that the morphology of the tributary drainages and slopes adjacent to the westernmost Grand

Canyon must be younger than the 17 Ma Grand Wash escarpment. They also noted that the beveling of the Hualapai Plateau indiscriminately across lithologies is indicative of a long-lived base level incompatible with a long lived paleo-Grand Canyon. A third conclusion is that a 70 Ma westernmost Grand Canyon requires improbably low erosion rates of ~4 m/m.y. maintained for tens of millions of years.

The "Muddy Creek constraint" is based on sediments from Grand Wash Trough, at the mouth of the Grand Canyon, that contain limited or no Colorado Plateau detritus and no far-traveled gravels from a pre-6 Ma Colorado River; instead, this area was internally drained prior to 6 Ma (Longwell 1946; Blackwelder, 1934; Lucchitta, 1966; 1972). More recent support for the Muddy Creek constraint comes from the geometry of the Miocene Pearce Canyon fan deposited across the modern path of the Colorado River (Lucchitta, 2013), and by detrital zircon data from siltstones near the mouth of the Grand Canyon that show no far-traveled sediment from the Colorado Plateau or Grand Canyon between 13 and 7 Ma (Crossey et al., 2015). Each of these lines of evidence refutes an "old" deeply carved canyon that followed the path of the westernmost Grand Canyon.

3. Procedures and parameters of thermochronologic modeling

Thermal history models were calculated incorporating data from multiple thermochronometers using HeFTy software (v. 1.8.3) (Ketcham, 2005), with constraints based on the best understanding of the geologic history of the sampled rocks (Figure 2). We assumed a surface temperature of 20±10°C, which spans the range of surface temperatures assumed in published studies for this region. All thermal models assumed the Radiation Damage Accumulation and Annealing Model (the RDAAM; Flowers et al., 2009), which quantifies He

186 diffusivity in apatite through geologic time. The RDAAM accounts for the effects of radiation
187 damage concentration on helium diffusivity in apatite (Shuster et al, 2006) by assuming the
188 annealing behavior of fission tracks can be used as a proxy for alpha-recoil damage annealing
189 (Flowers et al., 2009).

190 For many of our samples the ages appear to be over-dispersed (Vermeesch, 2010) and we
191 were unable to find time-temperature paths that predict the observed AHe ages within error. The
192 issue of age dispersion is a problem faced by other thermochronology studies (e.g. Vermeesh,
193 2010) that needs to be better addressed by the apatite thermochronology community. In our case,
194 in order to attempt to account for over-dispersion, we increased the measured uncertainty
195 proportionally until we were able to find time temperature paths that could explain the data,
196 which is equivalent to lowering the p-value and accepting more paths (Vermeesch and Tian,
197 2014). Over-dispersed ages may arise because uncertainty in AHe ages is estimated using the
198 high precision of the He, U and Th molar abundance measurements. These "analytical"
199 uncertainties that do not incorporate additional uncertainties, such as: corrections for alpha
200 ejection that do not account for the true shape of the crystal or the spatial distribution of U and
201 Th (Ault and Flowers, 2012), possible undetected micro inclusions (Farley and Stockli, 2002), or
202 neighboring minerals leading to alpha - injection (Spiegel et al., 2009). Therefore, the reported
203 "analytical" error likely underestimates system uncertainties. Other assumptions in the models
204 used to interpret the data may also not account for the true complexity of the system. For
205 example, Cl content may control the temperature and rate of radiation damage annealing
206 (Carlson et al., 1999; Donelick et al., 2005; Gautheron et al., 2013) and this is not accounted for
207 in RDAAM. Therefore, when discussing "good" and "acceptable" paths below, these are in
208 relation to the data with additional uncertainty included that attempts to account for the over-

dispersed ages. For complete transparency, a comparison of predicted ages and corrected ages are therefore shown for each model result figure.

Constraint boxes (Figure 2) were defined by potassium feldspar $^{40}Ar/^{39}Ar$ thermochronology data from McDermott (2011) and the known geologic history of the region (DR-6). Because all apatites are from Proterozoic basement rocks near river level, t-T paths began during the Precambrian and cooled to near-surface temperatures by Cambrian time beneath the Great Unconformity, with depth of near-surface residence thereafter determined by deposition and erosion of Paleozoic (~ 1 km) and Mesozoic (~ 2 km) strata. Flowers and Farley (2012) modeling of AHe data assumed that apatites were completely reset, and radiation damage was annealed, at temperatures of 110-120 °C at 80-100 Ma, just before the Laramide orogeny, and therefore began their thermal history models at these t-T conditions. However, long-term low-temperature residence of apatites between the Cambrian and the Laramide in our modeling allows for extensive pre-Laramide accumulation of radiation damage in the model, which may or may not have been completely annealed by Laramide burial (Fox and Shuster; 2014), and our broader 40-140 °C Laramide constraint box allow the data themselves to determine maximum Laramide burial temperatures.

In addition to reanalyzing the key sample (#2) from the Flowers and Farley (2012) study, we pursue a multi-sample approach to test geologic evidence for spatially variable thermal histories during progressive north-to-south cooling (Flowers, 2008) due to cliff retreat (Karlstrom et al., 2014; 2016), Laramide reverse and Miocene normal faulting (Huntoon et al. 1981, 1982), and the formation of older paleocanyon segments (Kelley et al., 2001; Young and Hartman, 2014; Karlstrom et al., 2014). These geologic factors argue against the assertion of Flowers et al. (2015) that “all western Grand Canyon samples have the same thermal history”.

Instead, we consider samples and data types individually before synthesizing the thermochronology of westernmost Grand Canyon relative to the geologic evidence outlined above.

Throughout this paper, we assume average surface temperatures of 25 ℃ and a geothermal gradient of 25 ℃/km (Wernicke, 2011). Estimates of the surface temperature for westernmost Grand Canyon range between 10-25 ℃ (average surface temperature in Death valley is 25 ℃), whereas geothermal gradient estimates are between 18-30 ℃/km; these estimates are generally based on well log and heat flow data summarized by Wernicke (2011). The assumptions of Wernicke (2011) and Flowers and Farley (2008) provide a reasonable 'minimum' value for a paleodepth estimate given the relatively high surface temperature estimate. However, these assumptions regarding the inversion of temperature to burial depth represent a major uncertainty in any thermochronologic study that involves estimating burial depth from temperature. These values undoubtedly vary by location and through geologic time in ways that are not quantifiable. Variables that have undetermined effects on surface temperatures and geothermal gradients through time and space include changes in the climate, elevation, and mantle temperatures; variations in thermal conductivity as strata are deposited and eroded; and the transient flow of groundwater. Complexities of how isotherms mimic topography in cases of ragged cliff retreat and/or below the edge of Music Mountain paleovalleys may also result in variations in the geothermal gradient. Thus, given the wide variation in published surface temperature and geothermal gradient assumptions compiled in Supplementary Table 2 of Karlstrom et al., (2014), thermochronology-determined paleodepths remain approximate and represent a continued uncertainty in geologic interpretations of thermal history models. While it is worth acknowledging these variables as a major uncertainty in our depth estimates, it is

beyond the scope of this paper to attempt to quantify the many effects of these variables. For the purposes of this study, it is enough to recognize that for a t-T path to be compatible with the proposed model of an "old" westernmost Grand Canyon cut to within 200 m of its modern depth (Wernicke, 2011), t-T paths must reach ~30 °C by 70-50 Ma, using the above assumptions. In contrast, modeled temperatures of ~ 40° C are interpreted to reflect ~ 600 m burial, the elevation differential between the river and present south rim in the westernmost Grand Canyon. Use of any higher geotherm or lower average surface temperature increases the interpreted depth of burial.

4. New thermochronologic data and thermal history models

All new and some previously published data used in this study are reported in the supplementary files and data repository of this paper. New AFT ages and lengths are presented in DR-1. Chemical data indicate that apatites from the westernmost Grand Canyon are dominantly fluoro-apatite, with low concentrations of Cl, indicating relatively rapid annealing of fission tracks. DR-2 presents new $^{4}He/^{3}He$ data, DR-3 presents published AHe data with errors and uncorrected ages (back-calculated in the case of Lee et al., 2013), DR-4 presents new AHe data, and DR-5 presents all goodness-of-fit (GOF) data and modeling parameters used for the thermal history models done in this study. Supplementary figures, including modeled thermal histories of published AHe data, are shown in DR-6 and a detailed summary of methodology and model results is presented in DR-7.

Each of the t-T path diagrams generated using HeFTy software shows the imposed t-T constraint boxes that are based on geologic observations, the good and/or acceptable t-T paths, and a gray bar that indicates the range of surface temperatures that need to be reached by 50 Ma

278 to support the "old" Canyon hypothesis. "Good" paths are designated by a goodness-of-fit (GOF)
279 of p=0.5 or greater and are shown in pink, while "acceptable" paths have a GOF of 0.05<p<0.5
280 and are shown in green, where p is the probability that the chosen path is not randomly selected
281 and in fact, represents the data in question. Per the user manual for HeFTy v.1.8.4, the relative
282 statistical fitting of good vs. acceptable paths implies that a "good" t-T path is supported by the
283 data, while an "acceptable" t-T path is not ruled out by the data.
284

Sample Number	**River Mile**	**Sample ID**	**Data source**	**Source rock description (Karlstrom et al., 2003)**	**AHe age range (Ma)**	**eU range (ppm)**	**# of AHe ages**	**AFT age**	**AFT lengths**
1	240	10GC161	***this study***	Separation pluton: weakly foliated, medium-grained granite; 1.71-1.68 Ga	55.3-93.4	1.1-14.6	4	60.8±4.4	13.1±1.6 (102)
2	240	CP06-69	Flowers et al., 2008, 2012	Separation pluton: weakly foliated, medium-grained granite; 1.71-1.68 Ga	64-76	11-13	5	--	--
3	243	01GC86	Lee et al., 2013	245-mile pluton: weakly foliated granodiorite; 1.73 Ga	29-72	10.6-17.1	3	62.8±4	13±0.4 (67)
4	245	10GC164	***this study***	245-mile pluton: weakly foliated granodiorite; 1.73 Ga	66.9-94.9	7.2-18.7	6	72.2±5.9	13.1±1.6 (92)
S1	245	CP06-71A	Flowers et al. 2008	245-mile pluton: weakly foliated granodiorite; 1.73 Ga	48-55	5-14	4	--	--
5	252	01GC87	Lee et al., 2013	Surprise pluton: granite; 1.7 Ga	69.5-90.1	81.8-231.7	6	68.7±3.8	12.1±0.4 (101)
S2	~252	GC863	Flowers and Farley, 2012	Surprise pluton: granite; 1.7 Ga	54-71	47-85	6	--	--
6	260	MH10-260	***this study***	Quartermaster pluton: megacrystic non-foliated granite; 1.35 Ma	15-71	3-34	4	63.2±7	12.3±2 (5)
7	225	04GC138	***this***	Diamond Creek	--	--	--	114±6.5	13.3±2.4

			study	pluton: granodiorite; 1.73 Ga					(66)
S3	225	04GC139	***this study***	Diamond Creek pluton: granodiorite; 1.73Ga	--	--	--	112±6.1	13.6±2.2 (47)
8	225	CP06-65	Flowers et al., 2008	Diamond Creek pluton: granodiorite; 1.73 Ga	51-81.4	32.48	4	--	--
9	230.5	MH10-230.5	***this study***	Travertine Falls pluton: medium-grained granite; 1.7 Ga	--	--	--	69.0±6.2	12.8±2.1 (101)

Table 1: Summary of thermochronologic data modeled in this study

4.1 Sample #1, Separation Canyon (RM 240): Combined AFT, AHe, and ^{4}He/^{3}He data

Sample # 1 (10GC161) is a new sample collected in the same location as sample #2 (CP06-69) from Flowers et al., 2008 and Flowers and Farley, 2012, which was the single key sample with interpretable ^{4}He/^{3}He and AHe data that led to their "old" Canyon conclusion. We applied all three complementary apatite thermochronology methods to this new sample. This section highlights initial inconsistencies in t-T paths derived from different thermochronologic data types in this location and throughout the westernmost Grand Canyon. Thermal history modeling was initially unable to produce any good or acceptable t-T paths when all three datasets (AHe, AFT, and ^{4}He/^{3}He) were combined after ~500,000 random tested paths for sample #1 (10GC161). Thus, we modeled the datasets independently (Figure 3 and Supplementary Figure 1) to generate viable t-T paths and then compared these t-T paths for both sample #1 and sample #2 (Figure 4A). Our reconciliation of all data into a single thermal history by modifying modeling parameters is presented after informative exploration of the separate datasets.

Bulk AHe ages for both sample #1 and #2 (age range 55.3-93.4 Ma and 64-76 Ma, respectively; Table 1), considered on their own, can be predicted by "old" Canyon t-T paths that

cool in a single event to near surface temperatures (~ 30°C) by ~70 Ma, in apparent agreement with Flowers and Farley (2012). AFT data from sample #1 (age of 60.8 Ma) are best predicted by t-T paths that cool gradually from peak Laramide temperatures of 100-140 °C to reach surface temperatures after 20 Ma and prefer a "young" Canyon. However, even with track length data, these AFT data alone are relatively insensitive to the <60 °C part of the t-T path where the controversy lies.

Figure 3 shows high-precision $^{4}He/^{3}He$ data obtained from sample #1, apatite A (Figure 3A), and our new model of $^{4}He/^{3}He$ data from sample #2 using our constraint boxes and the published U and Th zonation profiles for apatites C and D as model inputs (Figure 3B). The increased precision of $^{4}He/^{3}He$ data from sample #1 is due to higher ^{4}He concentration, derived from both larger crystal size and slightly higher U and Th concentrations. Accurate $^{4}He/^{3}He$ modeling requires knowledge of both the measured age and the U and Th zonation profile of an apatite crystal; unfortunately only one or the other can be measured on the same crystal as a consequence of the destructive nature of each measurement. Flowers and Farley (2012) measured zonation for sample #2 and used an assumed age of ~85 Ma (corrected) based on the mean age of four other apatite grains in the sample that had been previously analyzed (Flowers et al., 2008). Conversely, we measured the age of apatite A of sample #1 (93.4 Ma, corrected) and assumed no zonation in our modeling of this data, based on minimal zonation present in other crystals from this rock seen in the distribution of fission tracks and further analysis in the companion paper Fox et al. (in press; see Supplementary Figure 2 and Flowers and Farley, 2012).

$^{4}He/^{3}He$ data for sample #1 are best predicted by "young" Canyon t-T paths shown in Figure 3A and 3C. These paths show two-stage cooling: from 75 °C to ~60 °C at ~80 Ma, long-

term residence at ~55 °C, and then cooling to surface temperatures after 5 Ma. For comparison, an approximate 'old' Canyon path from Flowers and Farley (2012) (red lines in Figures 3A and 3C), does not predict the new $^{4}He/^{3}He$ data in Figure 3A. These new data alone therefore provide strong support for a "young" Canyon.

Figure 3D shows our new inverse modeling of sample #2 with $^{4}He/^{3}He$ data for two grains (C and D) using our constraint boxes that represent the complete thermal history and do not assume full annealing in the Laramide. The data are best predicted by t-T paths that reside at ~40 °C after the Laramide, although cooling still appears to be single-stage. We still interpret this as favoring a "young" Canyon because a temperature of 40 °C corresponds to a minimum of 600m of burial assuming a 25 °C surface temperature and 25 °C/km geothermal gradient, and does not support an "old" Canyon carved to within 200m of the modern depth at this location. Thus, both samples #1 and #2, when modeled using $^{4}He/^{3}He$ alone, favor a "young" Canyon and the uncertainty is whether rocks resided at ~ 55 °C (1.2 km) or ~40 °C (0.6 km) using the minimal depth conversion values of 25 °C and 25 °C/km.

Figure 4A shows a summary of the best-fit paths for samples #1 and #2 generated by independent modeling of the three types of datasets (AHe, AFT, and $^{4}He/^{3}He$) from the Separation Canyon location. Best-fit t-T paths from AHe data for both samples favor an "old" Canyon and are in striking disagreement with the thermal histories that best predict the $^{4}He/^{3}He$ data. Paths from the $^{4}He/^{3}He$ data and AFT data from sample #1 differ, but overlap near 50-60 Ma, the AFT age of this sample. For the Separation Canyon location, AFT and $^{4}He/^{3}He$ data, when modeled individually, are compatible with post-Laramide residence temperatures of 40-60 °C and a "young" Canyon whereas the t-T paths for the AHe data cool to near-surface temperatures by 70 Ma and are compatible with an "old" Canyon.

The importance of applying all methods to the same sample and of comparing two samples from the same location is that it is physically impossible for these apatites to have undergone different cooling histories. Our approach to reconcile all of the datasets is to favor the AFT and $^{4}He/^{3}He$ data, which agree best with the geologic evidence outlined earlier in this paper and provide better constraints on thermal history solutions due to the greater numbers of data in these measurements. For westernmost Grand Canyon, where the discussion is focused on the lowest temperatures of apatite sensitivity, AHe ages alone have limited resolution in comparison to $^{4}He/^{3}He$. $^{4}He/^{3}He$ data is also internally consistent as it originates from a single crystal, and is consequently subject to fewer variables and less uncertainty within the RDAAM. AHe ages from multiple crystals may be influenced by varying parameters per crystal that affect He diffusion kinetics (such as Cl content) that may not be accounted for by the RDAAM and therefore may not accurately predict the independent evolution of each crystal.

To account for uncertainty in the rate of alpha-recoil damage annealing, and its influence on He diffusivity, we adjust the r_{mr0} parameter in the RDAAM, following Fox and Shuster (2014). This empirically derived parameter links AFT annealing to alpha-recoil damage annealing and reflects the grain's resistance to annealing of radiation damage, which strongly influences He retentivity after reheating during sedimentary burial. Lower r_{mr0} values represent more retentive apatite that has a higher closure temperature range (Gautheron et al., 2013); thus AHe ages with lower r_{mr0} values are best predicted by higher temperature t-T paths. The RDAAM assumes a value of 0.83, which represents a typical fluorapatite's resistance to annealing; however values generally range between zero and one, with most values between 0.65 and 0.85, and often vary from apatite to apatite (Carlson et al., 1999; Ketcham et al., 1999; Ketcham et al., 2007). Figure 4B shows the effect of lowering r_{mr0} from the default value of 0.83

372 to 0.60 for a reference "young" Canyon path (Figure 4C) for the $^4He/^3He$ spectra of sample #2.
373 Lowering r_{mro} to 0.60 increases the GOF from 0.0 to 0.25 for grain c and from 0.0 to 0.16 for
374 grain d. This point was also made by Fox and Shuster (2014) using a different modeling
375 approach.

376 Figure 4D shows that all three datasets in sample # 1 (AHe, AFT, and $^4He/^3He$) can be
377 predicted by the same "young" Canyon t-T paths by adjusting the r_{mr0} values of individual AHe
378 ages. This required adjustment of the r_{mr0} values for AHe ages and relaxing the age uncertainties
379 to 10x the analytical error allowed the AHe ages, AFT age and lengths, and $^4He/^3He$ data to be
380 jointly modeled via the RDAAM, albeit with a poor GOF of 0.07. One AHe age (apatite X) was
381 excluded from this model as an old outlier on a positive age-eU trend given by the other apatites
382 Z, Y, and A (Supplemental Figure 1B). The t-T path from this final combined dataset (Figure
383 4D) shows a narrow set of 25 acceptable GOF paths after over 3 million total paths were tested.
384 These paths were only generated by varying r_{mr0} values for the different apatites to 0.70, 0.60,
385 and 0.60 for apatites A (with $^4He/^3He$ data), Z, and Y respectively. Other values for r_{mr0} for
386 apatite A were tried, but resulted in unrealistic values of r_{mr0} values (0.20 and lower) for the other
387 two apatites in order for t-T paths with acceptable GOF to be generated. Thus, our preferred
388 thermal history for sample #1 and the Separation Canyon location reaches burial temperatures of
389 90-120 °C during the Laramide, cools rapidly to residence temperatures of 40-50 °C, and reaches
390 surface temperatures after 5 Ma.
391

392 ***4.2 Combined (U-Th)/He and AFT models***

393 This section expands the thermochronologic coverage to other areas of the westernmost
394 Grand Canyon with the other samples, listed by river mile, in Table 1. We present new modeling

395 of previously published samples from Lee et al. (2013): sample #3 (01GC86, RM 243) and #5
396 (01GC87, RM 252) using our uniform model constraint boxes and new chemical data for the
397 AFT analyses. We also report new combined AFT and AHe analyses for sample # 4 (10GC164,
398 RM 245) and #6 (MH10-260, RM 260). Thermal histories for the jointly modeled datasets are
399 presented in Figure 5A-D.
400
401 *4.2.1 Sample # 3 (01GC86, RM 243); 245-mile granodiorite*
402 Figure 5A shows t-T paths that predict the combined AFT and AHe data from sample #3
403 (01GC86) from Lee et al. (2013). Three AHe ages range from 29-72 Ma, with a scattered age-eU
404 plot. Flowers et al. (2015) stated that this sample was "a problematic sample" because of high
405 dispersion of ages and a younger mean age (50 Ma) than other samples in the western Grand
406 Canyon and therefore should not be used for inversion modeling. In contrast, we see no reason to
407 reject this analysis as similar ages are found in several other samples and we have accounted for
408 unknown kinetic controls by increasing the estimated error for each age to achieve acceptable t-T
409 paths using the RDAAM. Our preferred best-fit path shows a single cooling episode to ~40 °C by
410 40-50 Ma from burial temperatures of 90-130 °C during the Laramide and cooling to near-surface
411 temperatures after ~20 Ma, similar to other thermal histories in this area. The thermal history
412 generated by modeling the three AHe ages alone for this sample without the AFT data remain
413 hotter, at ~70 °C, until after 20-30 Ma, when they cool to near-surface temperatures
414 (Supplementary Figure 3A). In this case, the addition of AFT to the AHe changes the modeled
415 thermal history for this sample from a "young" Canyon path to closer to an "old" Canyon path,
416 although neither path reaches near surface temperatures until after 20-30 Ma.
417

418 *4.2.2 Sample # 4 (10GC164, RM 245); Spencer Canyon pluton*

419 Figure 5B shows our preferred t-T path for the combined AFT and AHe data (5/6 grains)
420 for sample #4, which is at the same location as sample #S1 (CP06-71A from Flowers et al.,
421 2008; Supplementary Figure 4A). The AFT age for sample #4 is 72.2±5.9 Ma while the AHe
422 ages range from 66.9-94.6 Ma. HeFTy generated acceptable t-T paths only after the age error
423 was increased to 8x the analytical error. The best fit t-T path shows 100 °C peak burial
424 temperatures during the Laramide followed by cooling to ~40 °C by 60 Ma and no second stage
425 cooling. The model using AHe data alone for this sample (Supplementary Figure 3B) shows a
426 different t-T path using 3x the analytical error. These paths have a single stage of cooling from
427 ~80 °C during the Laramide to near surface temperatures of 20 °C, compatible with an "old"
428 Canyon. Thus, the AHe data alone predict an "old" Canyon whereas the combined AFT and AHe
429 t-T paths are not compatible with an "old" Canyon because near-surface temperatures are not
430 reached until after 20 Ma.
431
432 *4.2.3 Sample # 5 (01GC87, RM 252); Surprise Canyon pluton*
433 Figure 5C shows our preferred thermal history for this sample from Lee et al. (2013),
434 which is at the same location as sample #S2 (GC863 from Flowers and Farley, 2012;
435 Supplementary Figure 4B). Six AHe ages range from 69.5-90.1 Ma with a generally positive
436 age-eU slope; the AFT age is 68.7±3.8 Ma. The combined datasets are best predicted by a t-T
437 path showing a period of rapid cooling from ~90°C to ~60 °C during the Laramide, mid-Tertiary
438 slow cooling from 70 to 50 °C, and cooling to surface temperatures after 20 Ma. This suggests
439 ~1.4 km of burial after the Laramide and favors a "young" Canyon. AHe data modeled alone
440 (Supplementary Figure 3C) return a poorly constrained swath of t-T paths that in general show

cooling from 90-100 °C to ~40 °C during the Laramide before cooling gradually to surface temperatures, also favoring a "young" Canyon.

4.2.4 Sample #6 (MH10-260, RM 260); Quartermaster pluton

Figure 5D shows our preferred t-T path for this sample generated with combined AFT and AHe data. The AFT age is 63.2±7 Ma and four AHe ages range from 15-71 Ma with a strongly positive age-eU slope. This model generated acceptable GOF paths only after relaxing the estimated errors to 15x the reported analytical uncertainties. The best-fit path has a two-stage cooling history that reaches a maximum burial temperature of ~ 100 °C in the Laramide, cools between 85 and 70 Ma, and resides at ~50 °C through 70-10 Ma. The inflection showing onset of young cooling takes place after about 5 Ma. Similar thermal history models are generated by jointly modeling the 4 AHe analyses without the AFT data (Supplementary Figure 3D). The AHe t-T paths reach a slightly lower maximum burial temperature of ~80°C during the Laramide, cool and reside at ~60°C, and then reach surface temperatures after 10 Ma. Thermal histories for both the combined datasets and the AHe data alone support a "young" Canyon in that rocks remained at 50-60 °C until after 10 Ma, suggesting a minimum depth estimate of ~1km.

4.3 Samples # 7 and #8 from Diamond Creek: proof of concept for the paleocanyon hypothesis

The above data from westernmost Grand Canyon show that the combined thermochronologic data of $^{4}He/^{3}He$ (2 samples), AHe ages (6 samples) and apatite fission-track analyses (5 samples) are best predicted by t-T paths compatible with a "young" Canyon. The "old" Canyon hypothesis, which predicts cooling to within 200 m of the surface (30 °C) by 50 Ma, can be compatible with individual datasets but is not compatible with multi-method analyses

464 from any of the samples. Consequently, the westernmost Grand Canyon is a “young” segment,
465 carved in its present position in the past 5 Ma.

466 To test whether any segments of Grand Canyon are “old” as proposed by Karlstrom et al.,
467 2014, we analyzed samples # 7 (04GC138) and #S3 (04GC139) from Diamond Creek at RM 225
468 using AFT analysis. Diamond Creek a tributary to the Colorado River (Figure 1) where outcrops
469 of the 55-65 Ma Music Mountain Formation occur at relatively low elevations and Karlstrom et
470 al. (2014) and others (Young, 2001; Young and Hartman, 2014) have proposed that a ~60 Ma N-
471 flowing Paleocene river followed the Hurricane fault system. These samples are located near
472 each other (within 60 m) with minimal elevation difference, and were collected near river level
473 from the Diamond Creek pluton, at a similar location as sample #8 (CP06-65) from Flowers et al.
474 (2008). If the paleocanyon hypothesis of Karlstrom et al. (2014) is correct, these samples
475 represent an important proof-of-concept via their comparison to the westernmost Grand Canyon
476 and should have an “old” Canyon thermal history. Sample #7 (04GC138) has detailed Cl wt.%
477 and more track length measurements than sample #S3 (04GC139) and they are near enough to
478 each other that a similar thermal history is required, so only sample #7 was modeled although
479 data from both are presented in the data repository. The AFT age for sample #7 is 114.0±6.5,
480 older than the AFT ages for other samples considered in this study, and high uranium rims are
481 common in the analyzed apatites indicating some zonation. Figure 6A shows that AFT data for
482 sample #7 are predicted by a narrow suite of good GOF t-T paths that cool from ~90 °C to
483 surface temperatures by ~70 Ma. This single-stage cooling to surface temperatures supports that
484 an “old” ~60 Ma paleocanyon was present at this location, but based on comparison with the
485 westernmost Grand Canyon data it was the northern extension of the Music Mountain paleoriver
486 system and not carved by a paleo-Colorado River. Further support of low peak burial

487 temperatures in this region comes from the bimodal peak of AFT track lengths in Figure 6A and
488 6C.

489 Sample #8 (CP06-65) is a previously published sample from Flowers et al. (2008). This
490 sample is also from the Diamond Creek pluton at the same location near RM 225. Figure 6B
491 shows that all AHe ages from sample #8 can be predicted by t-T paths that cool rapidly from 80-
492 100 °C in the Laramide to temperatures of 30-60 °C before cooling gradually to reach surface
493 temperatures throughout the Cenozoic, a single-stage cooling history that is compatible with a
494 "young" Canyon at this location.

495 Figure 6C shows t-T paths that combine AHe ages from sample #8 with AFT data from
496 sample #7. Both are from the same location and must have had the same cooling history.
497 Predicted ages in the age-eU plot for this combined data thermal history model are much better
498 behaved than any other set of combined data in this region; the AFT age is significantly older
499 than the AHe ages and therefore can be accurately predicted by the RDAAM. The t-T paths that
500 result show a single stage of cooling in the Laramide, between 80 and 60 Ma, with rocks
501 reaching about 30 °C by 60 Ma, compatible with an "old" Canyon. For comparison, Figure 6D
502 shows t-T paths that predict AFT data from sample #9 (MH10-230.5, this study). The AFT age
503 for sample #9 is 69.0±6.2 Ma, similar to other AFT ages in the westernmost Grand Canyon but
504 much younger than the AFT ages for samples 7 and S3 at Diamond Creek. Sample #9's AFT t-T
505 paths cool gradually from peak temperatures of 90-140 °C during the Laramide over the entire
506 Cenozoic and reach surface temperatures after 20 Ma, compatible with a "young" Canyon.
507

508 **5. Discussion: reconciling dataset inconsistencies**

509 Figure 7 takes the weighted mean t-T paths from different samples and analytical
510 methods in order to compare modeling results. The results of the new analyses and new
511 modeling using uniform geologic constraints back to the Precambrian show that a preponderance
512 of these thermal histories, especially those that include combined datasets, support a "young"
513 westernmost Grand Canyon (yellow envelope). Four thermal histories constrained by AHe data
514 alone are best predicted by an "old" Canyon in Figure 7 but these paths are discordant relative to
515 all other paths, including paths from the same sample generated when the AHe data are
516 integrated with $^{4}He/^{3}He$ and/or AFT data from the same samples and same locations. These
517 disparate "old" and "young" Canyon t-T paths cannot both be geologically correct and must
518 result from limitations of the thermal history modeling; i.e. assumptions within the most current
519 model of apatite thermochronology systems behavior (the RDAAM) must not account for
520 important variables in an area of low-temperature burial reheating such as the westernmost
521 Grand Canyon.
522 In order to reconcile these discordant "old" Canyon AHe-only paths with the multi-
523 dataset "young" Canyon paths and the geologic data, we varied the value of r_{mr0} in the RDAAM.
524 The default value for the r_{mr0} parameter in the RDAAM assumes that alpha-recoil radiation
525 damage anneals at the same rate as fission track damage for a specific temperature. By
526 decreasing r_{mr0} within the range of its uncertainty (Ketcham et al., 2007), we assume that the rate
527 of annealing alpha-recoil damage is somewhat lower than fission track annealing in apatite (as
528 supported empirically; Ritter and Märk, 1986), which effectively increases the He retentivity of
529 each apatite grain after burial heating (Fox and Shuster, 2014). Since Laramide burial depths and
530 resulting temperatures (75-140 °C based on t-T paths from this study) may not have been
531 sufficiently high enough or endured for a sufficient time to completely anneal radiation damage

that accumulated during long-term surface residence, this assumed rate of radiation damage annealing is an especially important source of uncertainty in our analysis. This is partly addressed by requiring t-T paths to begin in the Proterozoic so the pre-Laramide thermal history can be accounted for, but cannot be totally reconciled between samples in this region using our current understanding of He diffusion in apatite.

During the modeling process, we noticed that the subset of t-T paths that reached higher temperatures during the Laramide (>110 °C) tended to reach cooler temperatures (<30 °C) more quickly than paths that stayed at lower temperatures, demonstrating the difference between starting modeled t-T paths at high temperatures in the Laramide such as those Flowers and Farley (2012) employed versus starting these paths in the Proterozoic to account for the entire thermal history and allowing the data to determine maximum burial temperatures. Fox and Shuster (2014) emphasized that when using the RDAAM, the t-T paths that represent AHe data are sensitive to the range of temperatures reached during maximum burial. These maximum burial temperatures are best constrained by AFT data and provide a valuable co-constraint that directly influence the t-T paths allowed by the AHe and $^{4}He/^{3}He$ data. The wide range allowed by our Laramide constraint box allows the AFT data to determine maximum burial temperatures and therefore pick the most representative low-T cooling paths following burial for the AHe data using the RDAAM; these t-T paths almost invariably support a "young" Canyon.

Figure 8 shows weighted mean paths for samples, color coded by river mile, to help evaluate whether different thermal history model results may reflect real variation in cooling histories. We interpret the "old" Canyon t-T paths at Diamond Creek to be real and to indicate that the Hurricane segment had cooled to 20-30 °C by 65-55 Ma and was carved by the Music Mountain and Hindu paleocanyon system (Karlstrom et al., 2014). Samples at river mile 240

555 (samples #1 and #2) reside at ~ 50 °C after the Laramide. Samples #3, #4, and #S1 in the
556 westernmost Grand Canyon have similar low-T post-Laramide residence of ~40 °C at river mile
557 243-246. Samples at river miles 250-260 (samples #5 and #6) reside at 60-80 °C after the
558 Laramide. These temperature differences could plausibly represent real differences in burial
559 depth. A geologic hypothesis capable of explaining different t-T paths in these locations involves
560 ragged cliff retreat of the Kaibab escarpment (Karlstrom et al., 2014). Figure 9 shows the
561 present-day position and an approximate 50 Ma position of this escarpment that could explain
562 different post-Laramide residence temperatures in westernmost Grand Canyon samples.
563
564 **6. Conclusions**
565 A diverse set of geologic studies continue to strongly support a 5-6 Ma integration of the
566 Colorado River from the Colorado Plateau to the Gulf of California and carving of the
567 westernmost Grand Canyon in the last 6 million years. The thermochronology of the
568 westernmost Grand Canyon has been controversial, but this paper demonstrates that the
569 thermochronology can be reconciled with compelling geologic field evidence. The application
570 of multiple thermochronology methods, especially new precise $^{3}He/^{4}He$ data, applied to the same
571 source rocks at Separation Canyon, resolves the debate about the age of westernmost Grand
572 Canyon. The combined data from this location cannot be explained by an "old" Canyon that was
573 carved to within 200 m of its modern depth by 50 Ma; indeed, the new $^{3}He/^{4}He$ data alone
574 precludes an "old" Canyon (see companion paper Fox et al., in press). Instead, our best t-T path
575 for this location involves two-stage cooling with both Laramide and < 10 Ma pulses. New t-T
576 paths generated by modeling other samples from this study, spanning river mile 230 to 260, also
577 argue strongly for a "young" westernmost Grand Canyon. In contrast, samples at RM 225 within

578 the Hurricane segment of Grand Canyon, are consistent with an “old” 55-65 Ma (Music
579 Mountain age) paleocanyon system that flowed north across the present path of the Grand
580 Canyon as proposed by Karlstrom et al. (2014).

581 Our best-fitting ‘young’ Canyon thermal history for westernmost Grand Canyon
582 involves: 1) a history of long term, low temperature residence since the Proterozoic (a key
583 difference between our models and previous models; e.g. Flowers and Farley, 2012); 2) peak
584 pre-Laramide burial temperatures of about 80-110 °C, compatible with burial by about 3 km of
585 Paleozoic and Mesozoic strata; 3) a Laramide cooling episode that took place from 90-70 Ma
586 and resulted in cooling to temperatures of 40-60 °C, compatible with erosional beveling of the
587 Hualapai Plateau to the level of the Esplanade Sandstone by the northward cliff retreat of a ~ 2
588 km section of upper Paleozoic and Mesozoic rocks; 4) a period of long-term (70 to 10 Ma)
589 residence at temperatures of 40-60 °C, compatible with burial of samples by about 1 km (600 m
590 to 1.4 km) of lower Paleozoic strata; this is consistent with the observed temporally persistent
591 fluvial base level observed on the Hualapai Plateau, and the absence of a westernmost Grand
592 Canyon; and 5) cooling to near-surface temperatures in the last 5-6 Ma, compatible with the
593 Muddy Creek constraint and the arrival of the Colorado River to the Gulf of California at about
594 5.3 Ma (Dorsey et al., 2007).

595 The westernmost Grand Canyon should continue to be an excellent field laboratory for
596 advancing understanding of low-temperature apatite thermochronology and He diffusion in
597 apatite with a complex thermal history. This study highlights a range of continued uncertainties
598 due to relatively low-temperature burial reheating where radiation damage may not be
599 completely annealed and involving complex He diffusion kinetics related to the rate and
600 temperature sensitivity of alpha-recoil damage annealing in apatite. Understanding possible

601 variables that control the retentivity of apatite crystals and variation in r_{mr0}, such as previously
602 unrecognized radiation damage effects, and better understanding of age dispersion in apatite
603 datasets are current challenges for modeling apatite thermochronology datasets.
604
605 **Acknowledgements**
606 Research was funded in part by NSF grant EAR- 1348007 and EAR- 1347990 (to Karlstrom and
607 Shuster) from the Tectonics Program. We acknowledge laboratory assistance provided by Nick
608 Fylstra. We thank two anonymous reviewers whose comments helped improve the paper.
609
610 **Figure captions**
611 Figure 1. A) Regional map showing geologic constraints and thermochronology sample locations
612 in westernmost Grand Canyon and the extent of Tertiary gravels and volcanic deposits across the
613 Hualapai Plateau, modified from Billingsley et al. (2006) and Karlstrom et al. (2014). Inset map
614 shows sections of the Grand Canyon. Pink star is the location of north-derived key Hindu
615 Fanglomerate exposure at head of Bridge Canyon. B) Google Earth image, looking SE,
616 highlighting the incision surrounding the Separation Point Basalt (SPb) and its source flow.
617 Geographic features are: BC= Bridge Canyon, CR= Colorado River, DC= Diamond Creek,
618 GWFZ= Grand Wash Fault Zone, GWC= Grand Wash Cliffs, HC= Old man-Hindu Canyon,
619 HFZ= Hurricane Fault Zone, HP= Hualapai Plateau, MF= Meriwhitica monocline and fault,
620 PSC= Peach Springs Canyon, SeC= Separation Canyon, ShP= Shivwits Plateau, SpC= Spencer
621 Canyon.
622

623 Figure 2. Constraint boxes imposed on models (using HeFTy v. 1.8.3) for all samples and their
624 geologic justifications. The long period of time that samples resided in and below the partial
625 retention zone between Precambrian and Laramide times may have resulted in extensive
626 radiation damage that was not fully annealed in the Laramide and hence produced complex and
627 variable He diffusion behavior in apatite.
628
629 Figure 3: New and previously published $^{4}He/^{3}He$ data from sample #1 (this paper) and #2
630 (Flowers and Farley, 2012) from the same location at Separation Canyon. A) New data (sample
631 #1) are more precise than prior data (#2) and are best predicted by the "young" Canyon t-T path
632 shown in black. B) Flowers and Farley (2012) data as modeled in this paper are also best
633 predicted by a "young" Canyon. C) Inverse thermal history model of apatite A from sample #1,
634 using the measured age of this grain (93.4 Ma) and assuming no zonation, returned a tightly
635 constrained "young" Canyon thermal history shown in black. D) Inverse thermal history model
636 of the Flowers and Farley (2012) data using the same AHe age and error that they used; note that
637 the ages for apatites C and D were not measured but were based on the mean AHe age (85.6 ±
638 6.8 Ma) and eU (12 ppm) from other AHe analyses for this sample (Flowers et al., 2008). The
639 good and best-fit paths support a "young" Canyon for both samples, but paths reside at ~40 ℃
640 (#2) instead of 50-60 ℃ (#1).
641
642 Figure 4: Reconciling the disagreement between Separation Canyon t-T paths. A) Best-fit t-T
643 paths from different analysis methods and samples (Sup. Fig. 1, Fig. 3) from the same location at
644 Separation Canyon show marked disagreement when modeled separately. B) To reconcile data,
645 we adjust the r_{mr0} value (a proxy for grain retentivity) in RDAAM using data from Flowers and

646 Farley (2012) to test a "young" Canyon reference path and find that assuming higher grain
647 retentivity by decreasing the r_{mr0} values to 0.6- 0.45 (red and blue curves) predicts the $^4He/^3He$
648 data with an acceptable GOF of 0.55- 0.97, respectively. C) Reference "young" Canyon path
649 used in B for varying r_{mr0}; inset of C shows blow up of the forward model after 120 Ma, the time
650 of interest for this study. D) By adjusting r_{mr0} values (different amounts for different samples, see
651 Supplementary data), RDAAM was able to predict all datasets together to return a suite of
652 acceptable t-T paths that reside at 40-50 °C after 70 Ma and reach surface temperatures after 5
653 Ma.
654
655 Figure 5: Samples with combined AFT and AHe data; age-eU plots and AFT track length GOF
656 are shown for each sample. A) Data from sample #3 are best predicted by a t-T path that cools to
657 ~40 °C during the Laramide. B) Data from sample #4 follow a similar cooling path as sample #3,
658 but are slightly warmer after the Laramide. C) Data from sample #5 have a 2-stage cooling
659 history; these paths stay at high temperatures (~60 °C) after slight cooling during the Laramide
660 and reach surface temperatures after 20 Ma. D) Data from sample #6 share a similar t-T path
661 with #5, but reside at ~50 °C and reach surface temperatures after 10 Ma.
662
663 Figure 6: The paleocanyon hypothesis of Karlstrom et al. (2014) suggests that samples from
664 Diamond Creek, because they are in the Hurricane segment, should give "old" Canyon t-T paths.
665 A) New sample (#7) from the same location as a key sample from Kelley et al. (2001) where
666 AFT data are best predicted by an "old" Canyon t-T path, consistent with this segment having
667 been carved by the ~ 55-65 Ma Music Mountain Formation system. B) Previously published
668 AHe data from Flowers (2008) from the same location as #7 that are best predicted by a "young"

669 Canyon t-T path. C) Combining our AFT (sample 7) with AHe data from sample #8 yields t-T
670 paths that reach surface temperatures by 60 Ma, compatible with the existence of a Music
671 Mountain paleocanyon. D) New AFT data from river mile 230.5, best predicted by a "young"
672 Canyon t-T path. Note the significant difference between this sample (#9) and sample #7.
673
674 Figure 7: A weighted mean t-T path comparison for all samples shows inconsistent paths.
675 Models using our new $^{4}He/^{3}He$ data, the $^{4}He/^{3}He$ data from Flowers and Farley (2012), all
676 models involving combined AFT and AHe, and about half the AHe-only t-T paths show post-
677 Laramide residence time at 40-60 ℃ from 70 to after 20 Ma, consistent with a "young" Canyon.
678 Four AHe-only best-fit paths are best predicted by t-T paths involving rapid cooling at 70 Ma,
679 consistent with an "old" Canyon (gray band). This range of t-T paths is not physically possible
680 because many of the conflicting t-T paths are from the same location. Our preferred path is the
681 jointly inverted multi-data set path from sample #1 (blue) suggesting that Separation Canyon
682 rocks reached maximum Laramide burial temperatures of 80-110 ºC, resided at post-Laramide
683 temperatures between 40-60 ℃ from 70 to 6 Ma, and cooled to near-surface temperatures after 5
684 Ma.
685
686 Figure 8: Synthesis of weighted mean t-T paths by river mile that shows preferred t-T paths
687 based on the combination of multiple analytical techniques. Our preferred path for each sample
688 is shown, including those with adjusted r_{mr0} values (RM 240). Most t-T paths support a "young"
689 Canyon, but post-Laramide residence T varies from 40-70 ºC. The black path is from samples #7
690 and #8 at Diamond Creek and suggests a paleocanyon carved by the Music Mountain paleoriver

691 along the Hurricane segment by ~60 Ma. Our preferred explanation for the varied post-Laramide
692 residence temperatures is ragged northward cliff retreat of the Kaibab escarpment.
693
694 Figure 9: A) Hypothesis that irregular scarp retreat of the Kaibab escarpment may explain
695 different post-Laramide (~ 50 Ma) residence temperatures of western Grand Canyon basement
696 samples. Paleocanyons at Diamond Creek and along the Hurricane segment of Grand Canyon
697 explain the cool temperatures of ~ 25 ℃ for the combined AFT and AHe data from samples 7
698 and 8 at ~50 Ma. In contrast, temperatures are ~50 ℃ at river mile 240 for samples #1 and #2, ~
699 40 ℃ for samples 3 and 4 at river miles 243-245, and ~60 ℃ at river miles 252-260, suggesting
700 variable cover by at least ~600 m of upper Paleozoic strata (assuming a 25 ℃ surface temperature
701 and 25 ℃/km geothermal gradient). Red outcrops are a shallowly emplaced Late Cretaceous
702 pluton, indicating appreciable cover at this location. Pink star is key exposure of Hindu
703 Fanglomerate sourced from northern exposures of Pennsylvanian-Permian strata. Paleochannel
704 flow directions and mapping are by Young and Crow (2014). B) N-S cross-section along line A-
705 A', using our preferred t-T path from sample #1 based on combined AFT, AHe, and $^{4}He/^{3}He$
706 data and assuming a 25 ℃ surface temperature and 25 ℃/km geothermal gradient to reconstruct
707 possible paleosurfaces above the Colorado River. This cross section includes surficial constraints
708 such as the Separation Point Basalt, Buck and Doe Conglomerate, north-derived Hindu
709 Fanglomerate, and Music Mountain Formation within the 55-65 Ma Hindu paleocanyon.
710
711
712 **Supplementary and data repository items**
713 DR-1 AFT summary, ages, and lengths

714 DR-2 New $^{4}He/^{3}He$ data

715 DR-3 Published apatite helium data

716 DR-4 New (U-Th)/He data

717 DR-5 Goodness-of-fit for the best-fit path in each model presented here relative to the data
718 entered.

719 DR-6 Supplementary figures

720 DR-7 Detailed methodology and results

721

722

723 **References cited**

724 Ault, A. K., & Flowers, R. M. (2012). Is apatite U–Th zonation information necessary for
725 accurate interpretation of apatite (U–Th)/He thermochronometry data? Geochimica et
726 Cosmochimica Acta, 79, 60–78. https://doi.org/10.1016/j.gca.2011.11.037

727 Babenroth, D.L., Strahler, A.N., 1945. Geomorphology and structure of the East Kaibab
728 monocline, Arizona and Utah. Bull. Geol. Soc. Am. 56, 107–150. doi:10.1130/0016-
729 7606(1945).

730 Billingsley, G.H., Block, D.L., Dyer, H.C., 2006. Geologic Map of the Peach Springs 30’x60'
731 Quadrangle, Mohave and Coconino Counties, Northwestern Arizona.

732 Blackwelder, E., 1934. Origin of the Colorado river. Bull. Geol. Soc. Am. 45, 551–566.
733 doi:10.1130/GSAB-45-551

734 Carlson, W.D., Donelick, R.A., Ketcham, R.A., 1999. Variability of apatite fission-track
735 anneling kinetics; I, Experimental results. Am. Mineral. 84, 1213–1223. doi:10.2138/am-
736 1999-0901

737 Crossey, L.J., Karlstrom, K.E., Dorsey, R.J., Pearce, J., Wan, E., Beard, L.S., Asmerom, Y.,
738 Polyak, V.J., Crow, R.S., Cohen, A., Bright, J., Pecha, M.E., 2015. Importance of
739 groundwater in propagating downward integration of the 6-5 Ma Colorado River system:
740 Geochemistry of springs, travertines, and lacustrine carbonates of the Grand Canyon region
741 over the past 12 Ma. Geosphere 11, 660–682. doi:10.1130/GES01073.1
742 Darling, A., Whipple, K.X., 2015. Geomorphic constraints on the age of the western Grand
743 Canyon. Geosphere 11, 1–19. doi:10.1130/GES01131.1
744 Davis, W.M., 1901, An excursion to the Grand Canyon of the Colorado: Harvard Museum of
745 Comparative Zoology Bulletin, v. 38, p. 106-201.
746 Donelick, R. A., O'Sullivan, P. B., & Ketcham, R. A. (2005). Apatite Fission-Track Analysis.
747 Reviews in Mineralogy and Geochemistry, 58, 49–94.
748 https://doi.org/10.2138/rmg.2005.58.3
749 Dorsey, R.J., Fluette, A., McDougall, K., Housen, B. a., Janecke, S.U., Axen, G.J., Shirvell,
750 C.R., 2007. Chronology of Miocene-Pliocene deposits at Split Mountain Gorge, Southern
751 California: A record of regional tectonics and Colorado River evolution. Geology 35, 57–
752 60. doi:10.1130/G23139A.1
753 Dutton, C.E., 1882. Tertiary history of the Grand Cañon District, Reprint, 1. ed. United States
754 Geological Survey, Santa Barbara, CA and Salt Lake City, UT.
755 Elston, D.P., Young, R. A., 1991. Cretaceous-Eocene (Laramide) landscape development and
756 Oligocene-Pliocene drainage reorganization of transition zone and Colorado Plateau,
757 Arizona. J. Geophys. Res. 96, 12389. doi:10.1029/90JB01978
758 Farley, K.A., Stockli, D.F., 2002. (U-Th)/He Dating of Phosphates: Apatite, Monazite, and
759 Xenotime. Rev. Mineral. Geochemistry 48, 559 LP-577.

760 Flowers, R.M., Farley, K.A., 2013. Response to Comments on "Apatite $^{4}He/^{3}He$ and (U-Th)/He
761 Evidence for an Ancient Grand Canyon". Science 340, 143. doi:10.1126/science.1234203
762 Flowers, R.M., Farley, K.A., 2012. Apatite $^{4}He/^{3}He$ and (U-Th)/He evidence for an ancient
763 Grand Canyon. Science 338, 1616–9. doi:10.1126/science.1229390
764 Flowers, R.M., Farley, K.A., Ketcham, R.A., 2015. A reporting protocol for thermochronologic
765 modeling illustrated with data from the Grand Canyon. Earth Planet. Sci. Lett. 432, 425–
766 435. doi:10.1016/j.epsl.2015.09.053
767 Flowers, R.M., Ketcham, R.A., Shuster, D.L., Farley, K.A., 2009. Apatite (U–Th)/He
768 thermochronometry using a radiation damage accumulation and annealing model. Geochim.
769 Cosmochim. Acta 73, 2347–2365. doi:10.1016/j.gca.2009.01.015
770 Flowers, R.M., Wernicke, B.P., Farley, K.A., 2008. Unroofing, incision, and uplift history of the
771 southwestern Colorado Plateau from apatite (U-Th)/He thermochronometry. Geol. Soc. Am.
772 Bull. 120, 571–587. doi:10.1130/B26231.1
773 Fox, M., Shuster, D.L., 2014. The influence of burial heating on the (U–Th)/He system in
774 apatite: Grand Canyon case study. Earth Planet. Sci. Lett. 397, 174–183.
775 doi:10.1016/j.epsl.2014.04.041
776 Fox, M., Tripathy-Lang, A, Shuster, D. L., Winn, C., Karlstrom, K., Kelley, S., in review.
777 Westernmost Grand Canyon incision: testing thermochronometric resolution.
778 Gautheron, C., Barbarand, J., Ketcham, R.A., Tassan-Got, L., van der Beek, P., Pagel, M., Pinna-
779 Jamme, R., Couffignal, F., Fialin, M., 2013. Chemical influence on α-recoil damage
780 annealing in apatite: Implications for (U-Th)/He dating. Chem. Geol. 351.
781 doi:10.1016/j.chemgeo.2013.05.027
782 Huntoon, P.W., Billingsley, G.H., Clark, M.D., 1981. Geologic map of the Hurricane Fault Zone

783 and Vicinity, Western Grand Canyon, Arizona.
784 Huntoon, P.W., Billingsley, G.H., Clark, M.D., 1982. Geologic map of the Lower Granite Gorge
785 and Vicinity, Western Grand Canyon, Arizona.
786 Karlstrom, K.E., Crossey, L.J., Embid, E., Crow, R., Heizler, M., Hereford, R., Beard, L.S.,
787 Ricketts, J.W., Cather, S., Kelley, S., 2016. Cenozoic incision history of the Little Colorado
788 River: its role in carving Grand Canyon and onset of rapid incision in the last ~2 Ma in the
789 Colorado River System. Geosphere.
790 Karlstrom, Karl E., Ilg, B.R., Williams, M.L., Hawkins, D.P., Bowring, S.A., Andseaman, S.J.,
791 2003, Paleoproterozoic rocks of the Granite Gorges, in Beus, S.S., and Morales, M., eds.,
792 Grand Canyon Geology: New York, Oxford University Press, p. 9–38.
793 Karlstrom, K.E., Lee, J.P., Kelley, S.A., Crow, R.S., Crossey, L.J., Young, R.A., Lazear, G.,
794 Beard, S.L., Ricketts, J.W., Fox, M., Shuster, D.L., 2014. Formation of the Grand Canyon 5
795 to 6 million years ago through integration of older palaeocanyons. Nat. Geosci. 7, 239–244.
796 doi:10.1038/NGEO2065
797 Kelley, S.A., Chapin, C.E., Karlstrom, K.E., 2001. Laramide Cooling Histories of Grand
798 Canyon, Arizona, and the Front Range, Colorado, Determined from Apatite Fission-track
799 Thermochronology 37–44.
800 Ketcham, R.A., 2005. Forward and Inverse Modeling of Low-Temperature Thermochronometry
801 Data. Rev. Mineral. Geochemistry 58, 275–314. doi:10.2138/rmg.2005.58.11
802 Ketcham, R.A., Donelick, R.A., Carlson, W.D., 1999. Variability of apatite fission-track
803 anneling kinetics: III. Extrapolation to geological time scales. Am. Mineral. 84, 1235–1255.
804 Ketcham, R.A., Carter, A., Donelick, R.A., Barbarand, J., Hurford, A.J., 2007. Improved
805 modeling of fission-track annealing in apatite. Am. Mineral. 92, 799–810.

806 doi:10.2138/am.2007.2281
807 Lee, J.P., Stockli, D.F., Kelley, S.A., Pederson, J.L., Karlstrom, K.E., Ehlers, T.A., 2013. New
808 thermochronometric constraints on the Tertiary landscape evolution of the central and
809 eastern Grand Canyon , Arizona. Geosphere 9, 216–228. doi:10.1130/GES00842.1
810 Longwell, C.R., 1946. How old is the Colorado River? Am. J. Sci. 244, 818–835.
811 Lucchitta, I., 1966, Cenozoic geology of the upper Lake Mead area adjacent to the Grand Wash
812 Cliffs, Arizona [Ph.D. thesis]: State College, Pennsylvania State University, 218 p.
813 Lucchitta, I., 1972. Early history of the Colorado River in the Basin and Range Province. GSA
814 Bull. 83, 1933–1948.
815 Lucchitta, I., Holm, R.F., Lucchitta, B.K., 2013. Implications of the Miocene (?) Crooked Ridge
816 River of northern Arizona for the evolution of the Colorado River and Grand Canyon.
817 Geosphere 9, 1417–1433. doi:10.1130/GES00861.1
818 McDermott, Jacob J., 2011. Microstructural, U-Th-Pb geochronologic and $^{40}Ar/^{39}Ar$
819 thermochronologic evidence for both Paleoproterozoic and Mesoproterozoic displacement
820 across the Gneiss Canyon shear zone: Lower Granite Gorge, Grand Canyon, Arizona
821 [Master's thesis]: University of New Mexico, 34 p.
822 McKee, E.D., Wilson, R.F., Breed, W.J., and Breed, C.S., eds., 1967, Evolution of the Colorado
823 River in Arizona: Museum of Northern Arizona Bulletin 44, 67 p.
824 Naeser, C.W., Duddy, I.R., Elston, D.P., Dumitru, T.A., Green, P.F., 1989. Fission-Track
825 Dating: Ages for Cambrian Strata and Laramide and Post-Middle Eocene Cooling Events
826 From the Grand Canyon, Arizona, in: Geology of Grand Canyon, Northern Arizona (with
827 Colorado River Guides): Lee Ferry to Pierce Ferry, Arizona. American Geophysical Union,
828 pp. 139–144. doi:10.1029/FT115p0139

829 Powell, J.W., 1875, Exploration of the Colorado River of the West and Its Tribu- taries:
830 Smithsonian Institution Annual Report, 291 p.
831 Ritter, W., Märk, T.D., 1986. Radiation damage and its annealing in apatite. Nucl. Instruments
832 Methods Phys. Res. Sect. B Beam Interact. with Mater. Atoms 14, 314–322.
833 doi:10.1016/0168-583X(86)90601-4
834 Shuster, D.L., Farley, K.A., 2005. $^{4}He/^{3}He$ Thermochronometry: Theory, Practice, and Potential
835 Complications. Rev. Mineral. Geochemistry 58, 181–203. doi:10.2138/rmg.2005.58.7
836 Shuster, D.L., Flowers, R.M., Farley, K.A., 2006. The influence of natural radiation damage on
837 helium diffusion kinetics in apatite. Earth Planet. Sci. Lett. 249, 148–161.
838 doi:10.1016/j.epsl.2006.07.028
839 Spiegel, C., Kohn, B., Belton, D., Berner, Z., Gleadow, A., 2009. Apatite (U–Th–Sm)/He
840 thermochronology of rapidly cooled samples: The effect of He implantation, Earth and
841 Planetary Science Letters. doi:10.1016/j.epsl.2009.05.045
842 Stevens, L., 1983. The Colorado River in Grand Canyon, a Guide. Flagstaff, AZ Red Lake
843 Books I 987.
844 Strahler, A.N., 1948. Geomorphology and structure of the West Kaibab fault zone and Kaibab
845 Plateau, Arizona. Bull. Geol. Soc. Am. 59, 513–540.
846 Vermeesch, P., 2010. HelioPlot, and the treatment of overdispersed (U–Th–Sm)/He data. Chem.
847 Geol. 271, 108–111. doi:10.1016/j.chemgeo.2010.01.002
848 Vermeesch, P., Tian, Y., 2014. Thermal history modeling : HeFTy vs. QTQt. Earth Sci. Rev.
849 139, 279–290. doi:10.1016/j.earscirev.2014.09.010
850 Warneke, N.L., 2015. Timing of erosional episodes in the Marble Canyon and Vermilion Cliffs
851 region from apatite (U- Th)/ He thermochronology [Master's Thesis]: University of New

852 Mexico, 69 p.
853 Wenrich, K.J., Billingsley, G., Blackerby, B.A., 1995. Spatial migration and compositional
854 changes of Miocene-Quaternary magmatism in the western Grand Canyon. J. Geophys. Res.
855 100, 10417–10440. doi:10.1029/95JB00373
856 Wernicke, B.P., 2011. The California River and its role in carving Grand Canyon. GSA Bull.
857 123, 1288–1316. doi:10.1130/B30274.1
858 Young, R.A., 1966, Cenozoic geology along the edge of the Colorado Plateau in northwestern
859 Arizona [PhD thesis]: Washington University, St. Louis, 167p.
860 Young, R.A., 2001, The Laramide-Paleogene history of the western Grand Canyon region:
861 Setting the stage, in Young, R.A., and Spamer, E.E., eds., Colorado River: Origin and
862 Evolution: Grand Canyon, Grand Canyon Association Monograph 12, p. 7–15.
863 Young, R. A, Crow, R.S., 2014. Paleogene Grand Canyon incompatible with Tertiary
864 paleogeography and stratigraphy. Geosphere 664–679. doi:10.1130/GES00973.1
865 Young, R.A., Hartman, J.H., 2014. Paleogene rim gravel of Arizona: Age and significance of the
866 Music Mountain Formation. Geosphere 1–22. doi:10.1130/GES00971.1
867

Click here to download Figure: WGCfigures FINAL 170417small.pdf

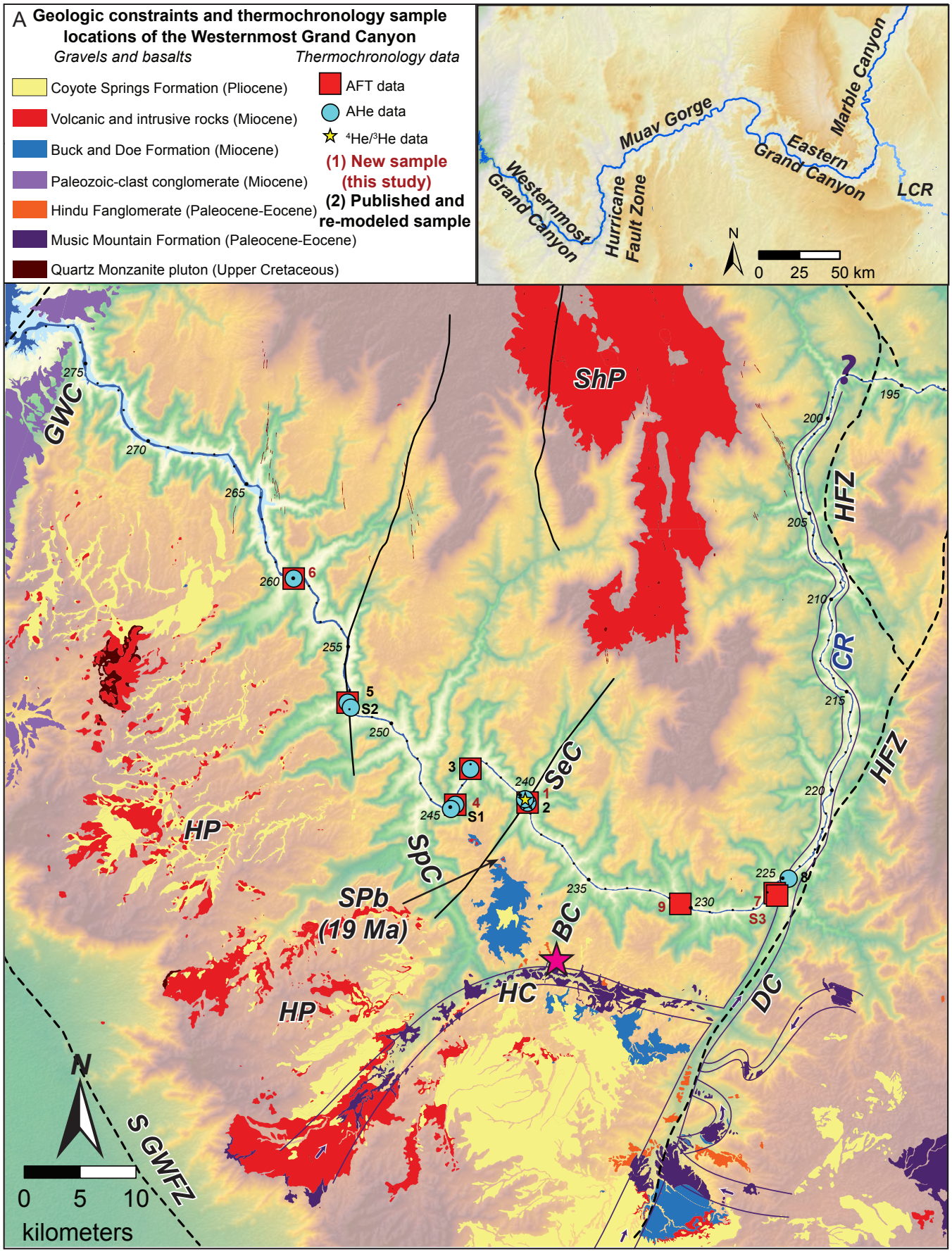

Winn et al. Figure 1

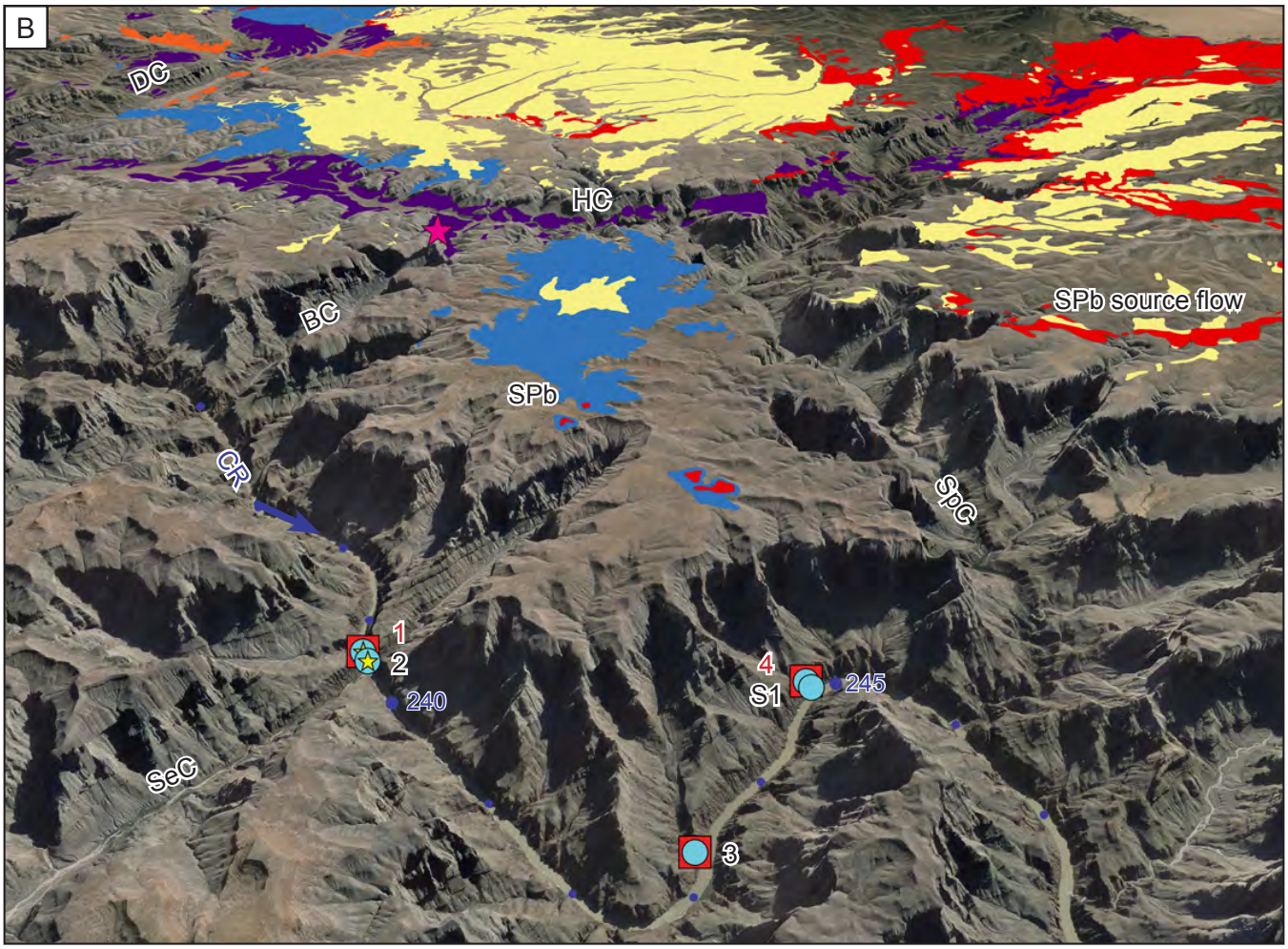

Winn et al. Figure 2

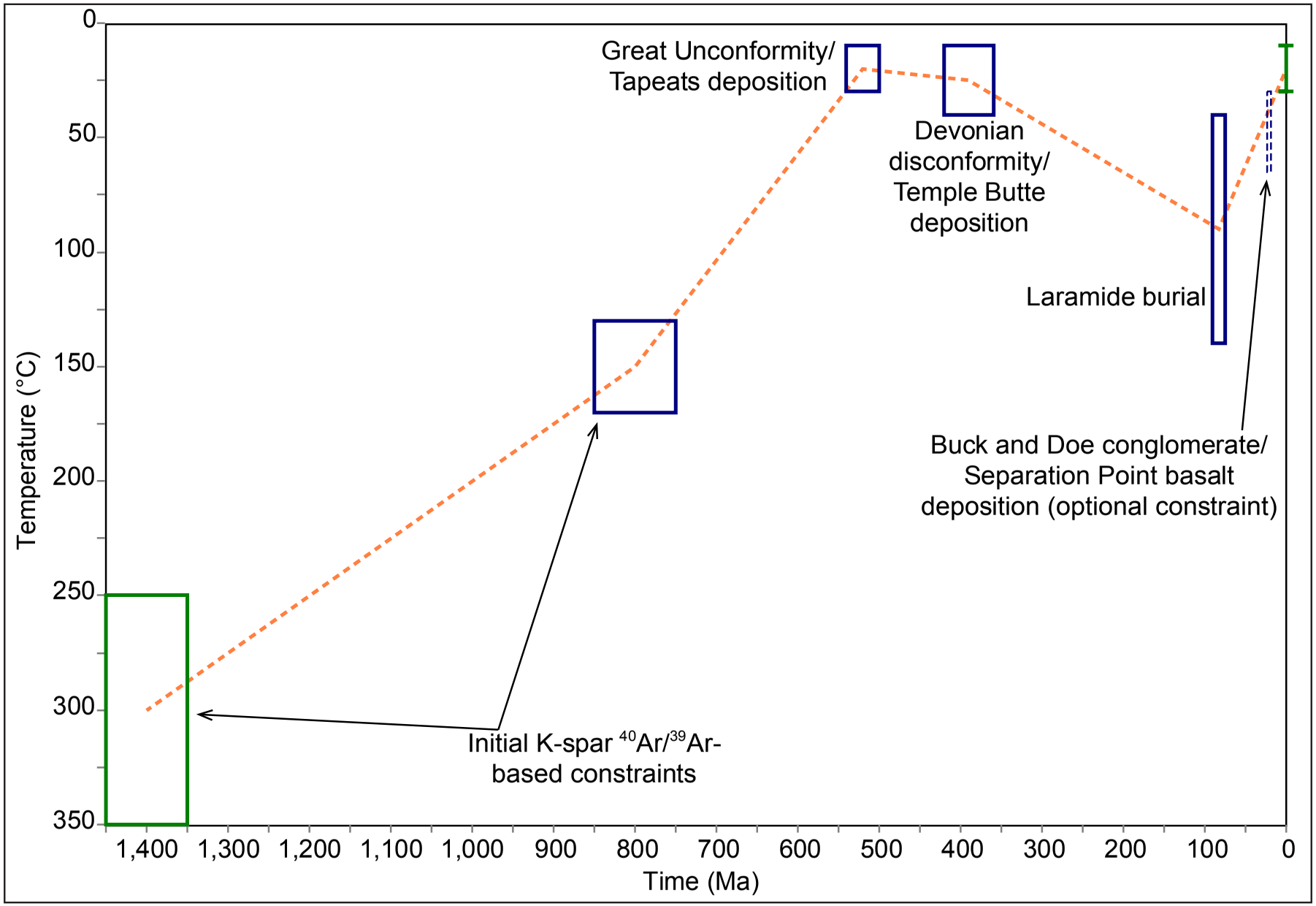

Winn et al. Figure 3

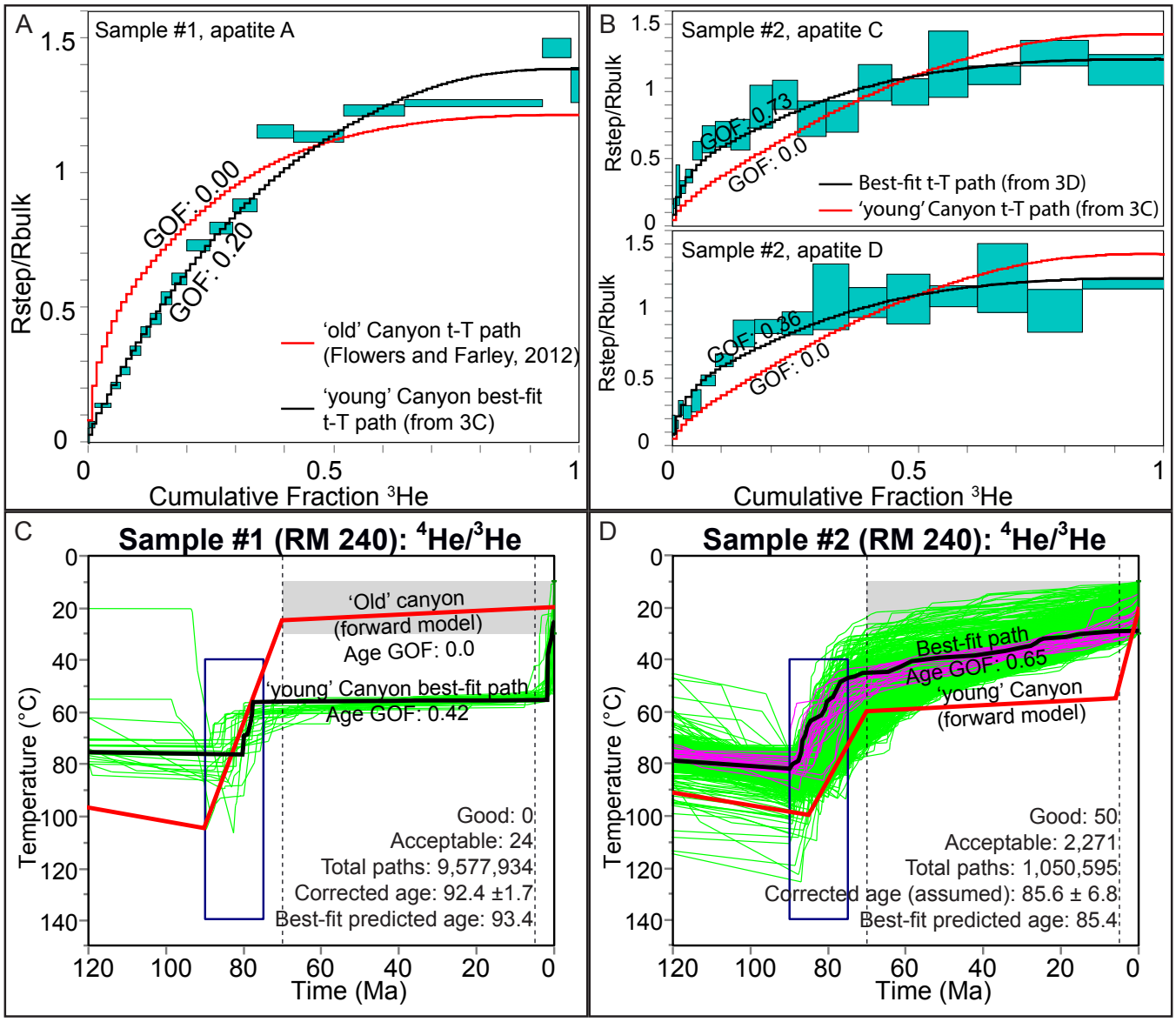

Winn et al. Figure 4

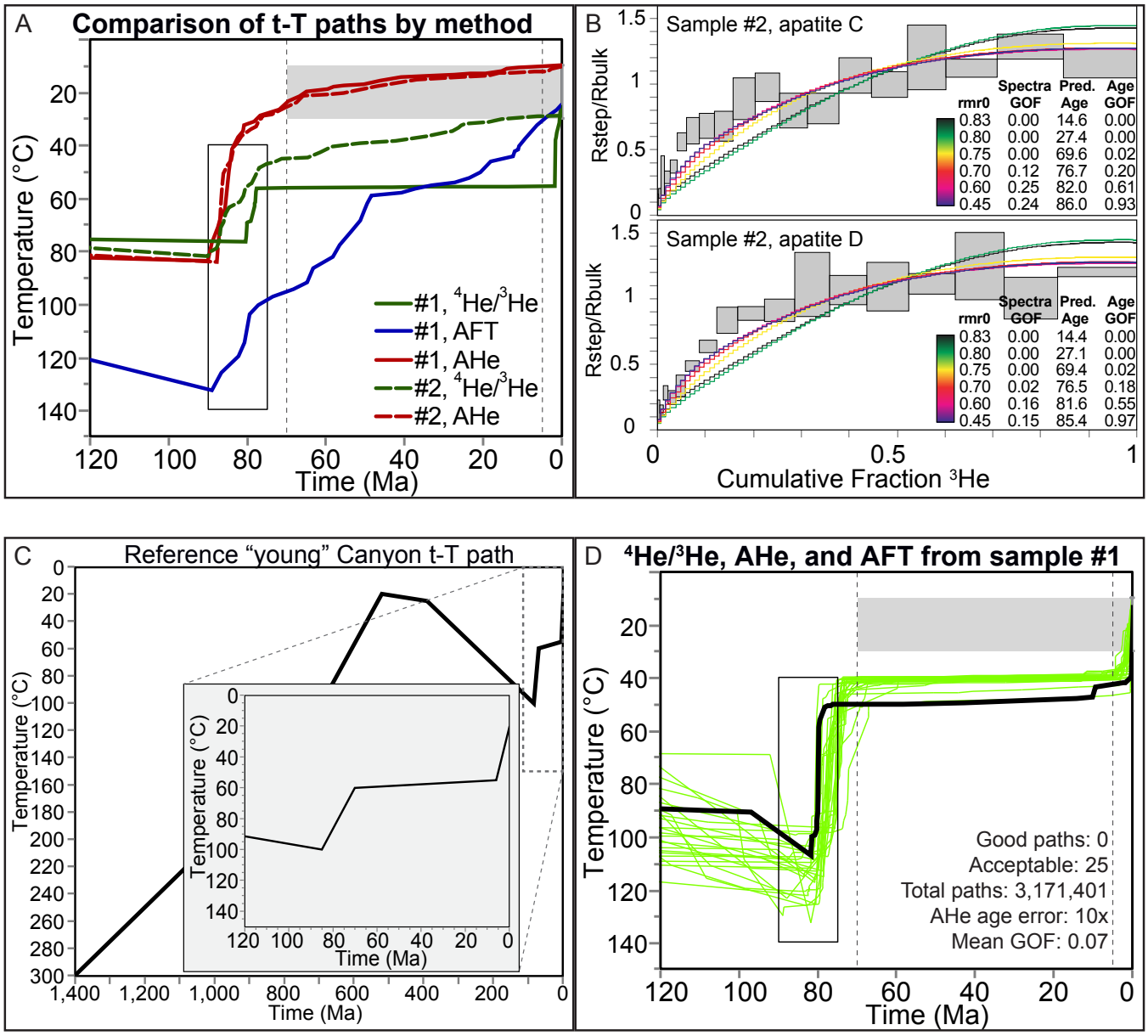

Winn et al. Figure 5

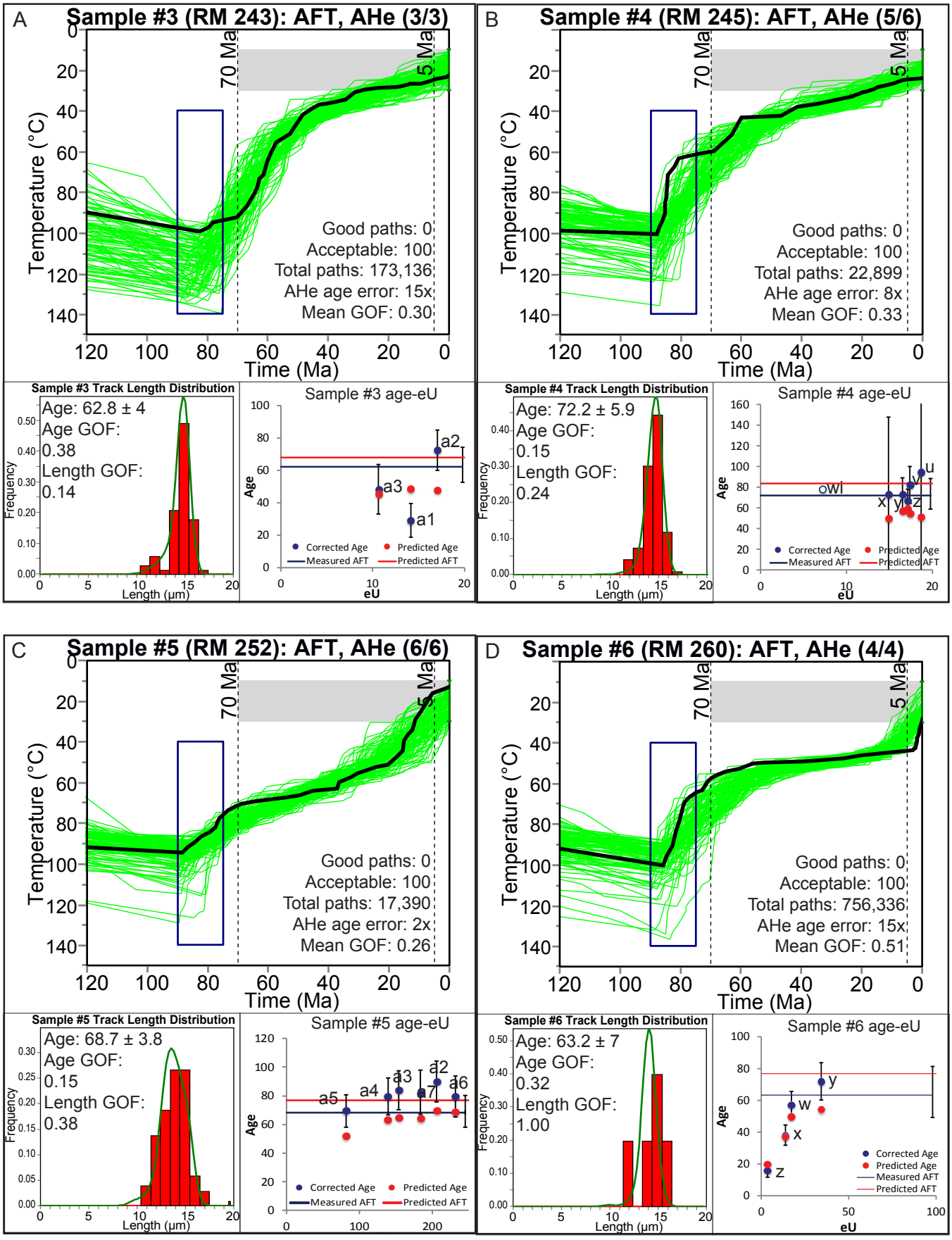

Winn et al. Figure 6

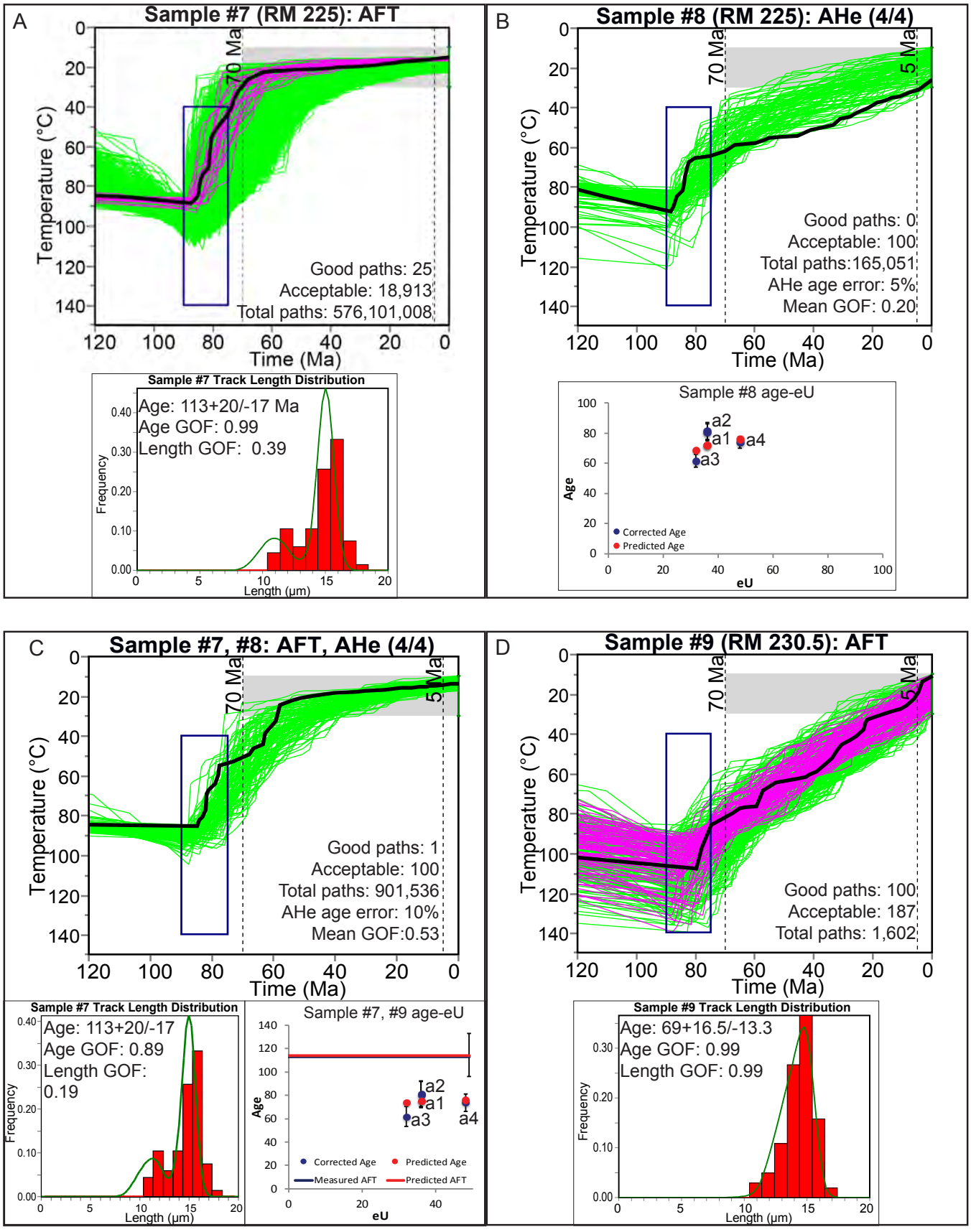

Winn et al. Figure 7

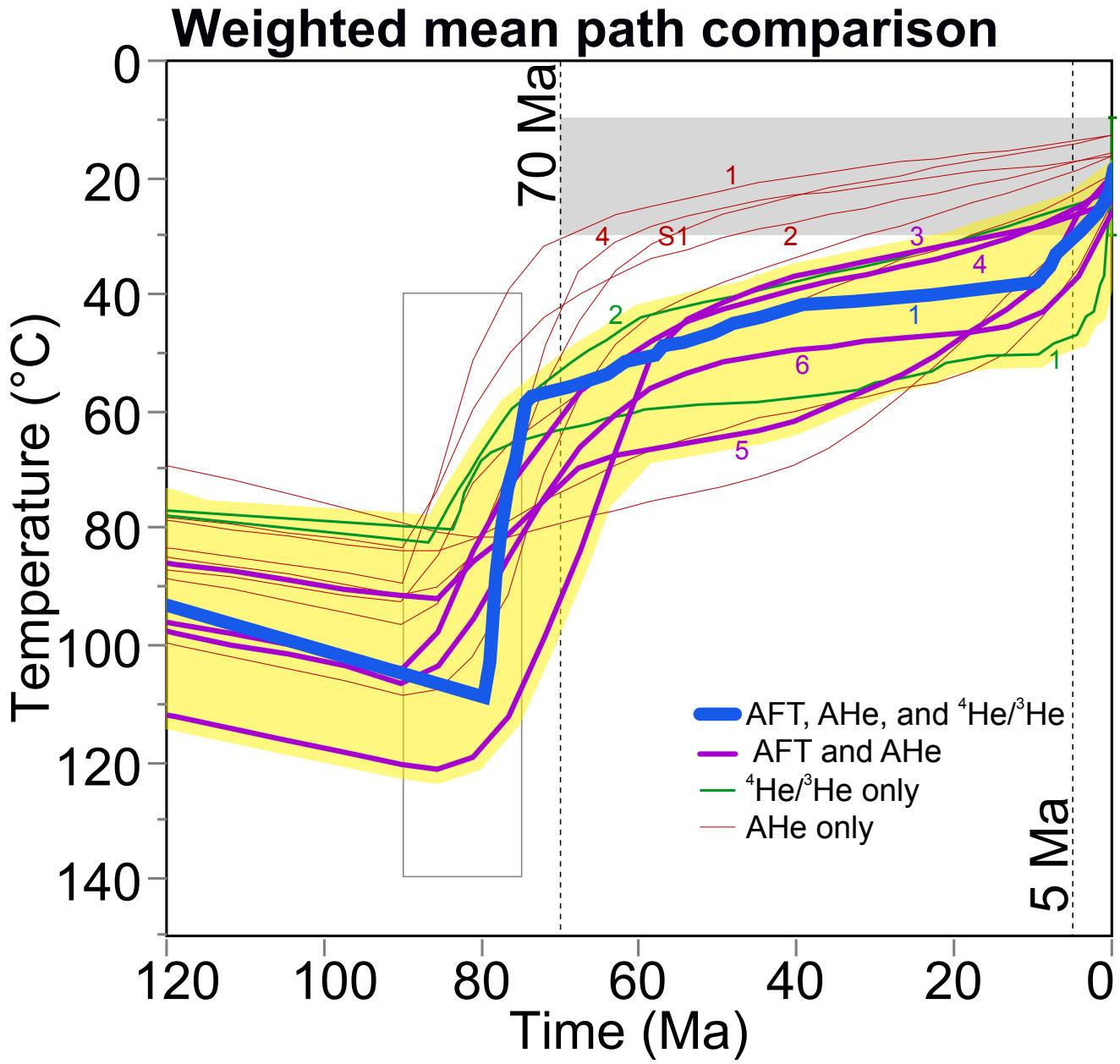

Winn et al. Figure 8

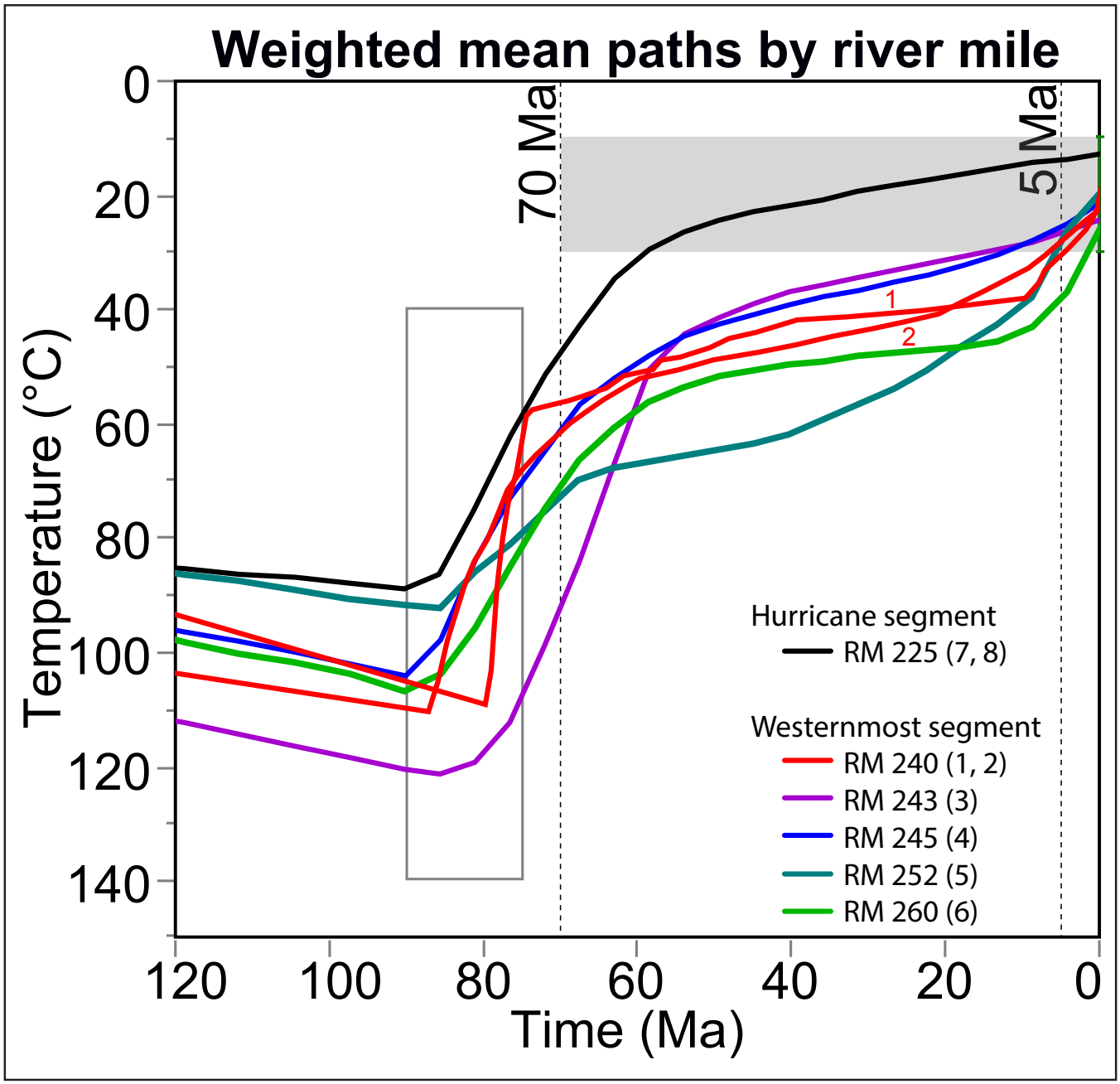

Winn et al. Figure 9

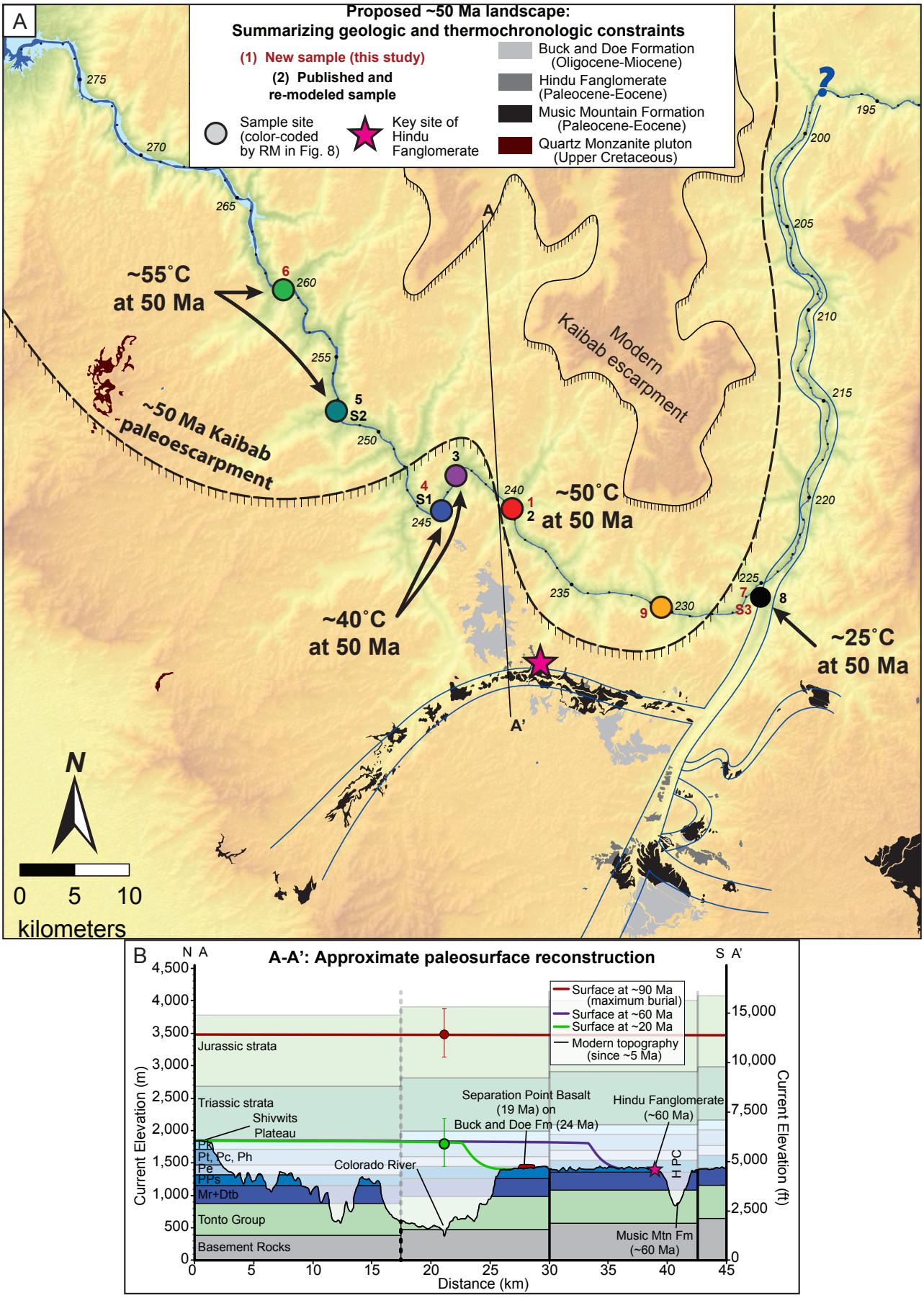

Figures - originally submitted

Click here to download Figure: WGCfigures 161115small.pdf

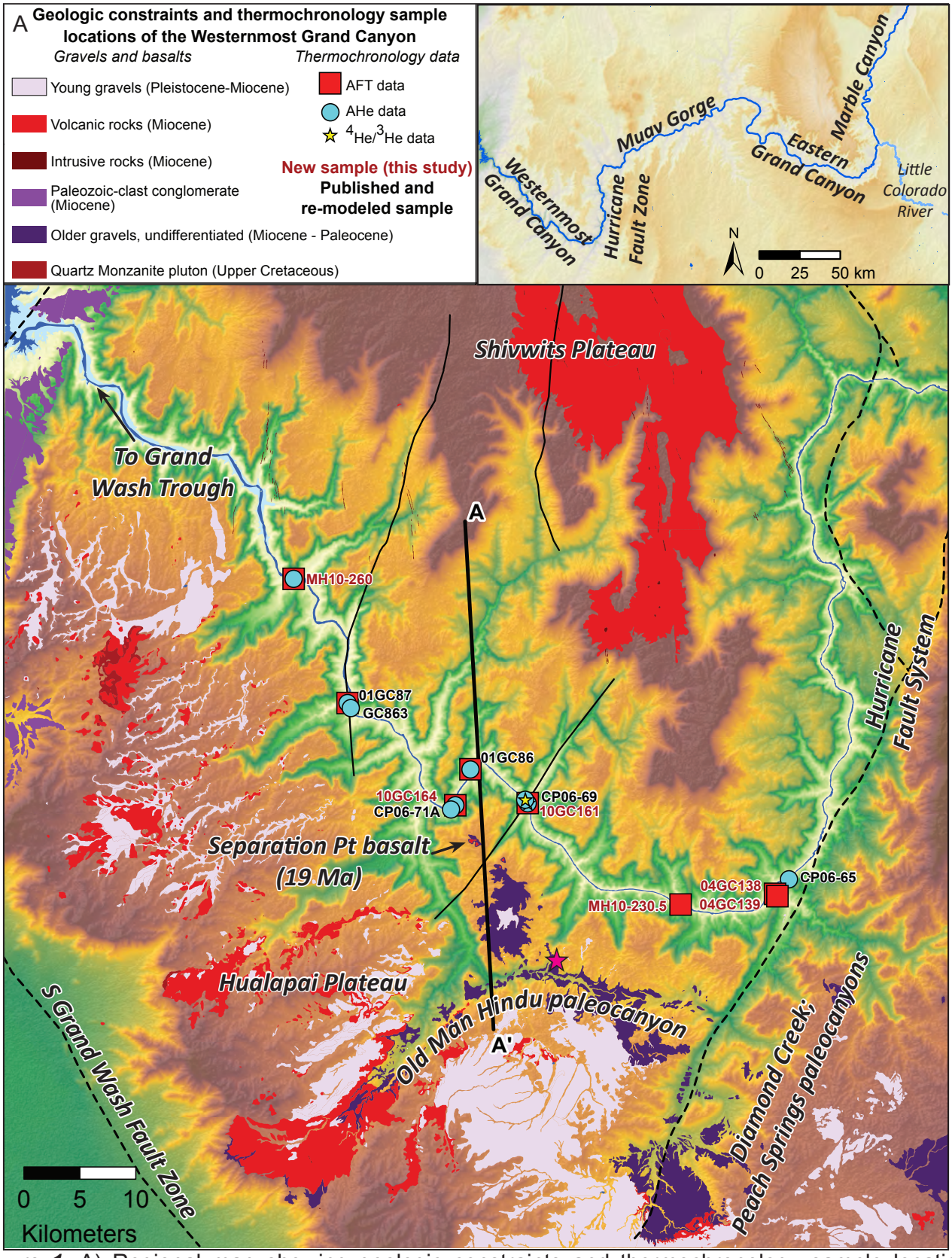

Figure 1. A) Regional map showing geologic constraints and thermochronology sample locations in westernmost Grand Canyon and the extent of Tertiary gravels and volcanic deposits across the Hualapai Plateau, taken from Billingsley et al. (2006). Miocene-Paleocene gravels are undifferentiated. Inset map shows sections of the Grand Canyon. Blue star is the location of the Hindu Fanglomerates.

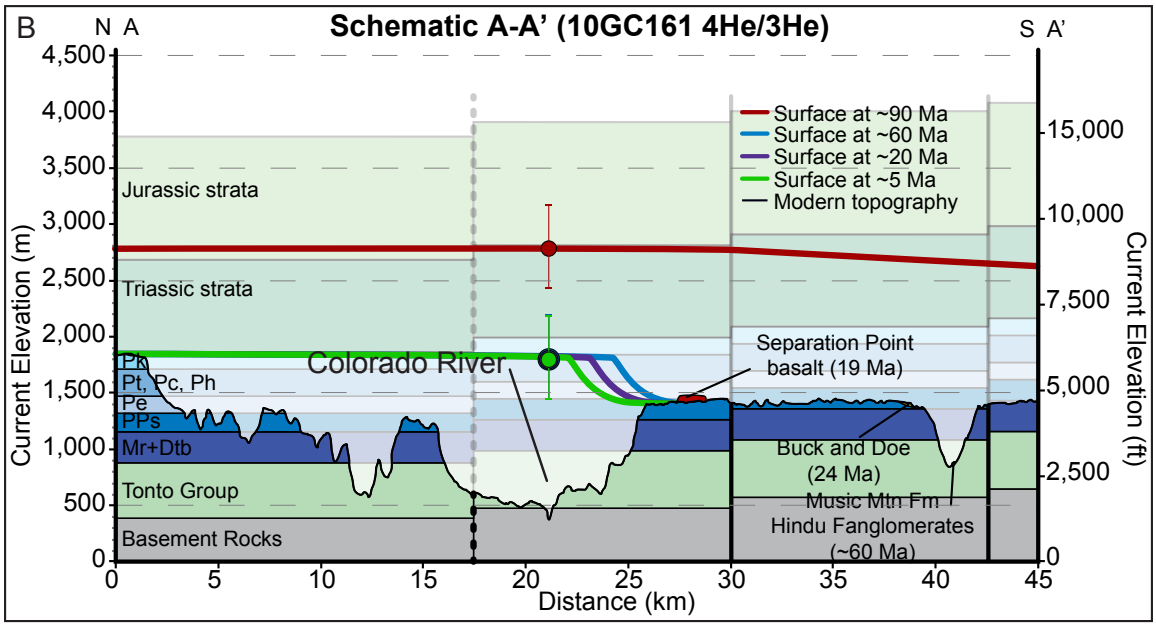

Figure 1, continued. B) Schematic cross section showing the relationships between the beveled surface of the Hualapai Plateau, the Music Mountain Formation in the Old Man Hindu paleocanyon, the Buck and Doe conglomerate, and the Separation Point Basalt. Location of cross section line A-A' is shown in Figure 1. Paleosurfaces were estimated from the best t-T path derived from $^{4}He/^{3}He$ data for sample 10GC161 at Separation Canyon assuming a 25˚C surface T and 25 ˚C/km geothermal gradient. Cliff retreat of lower Paleozoic strata to their present position on the north rim plus canyon carving resulted in ~35-50 ˚C of cooling in the last 5-6 Ma.

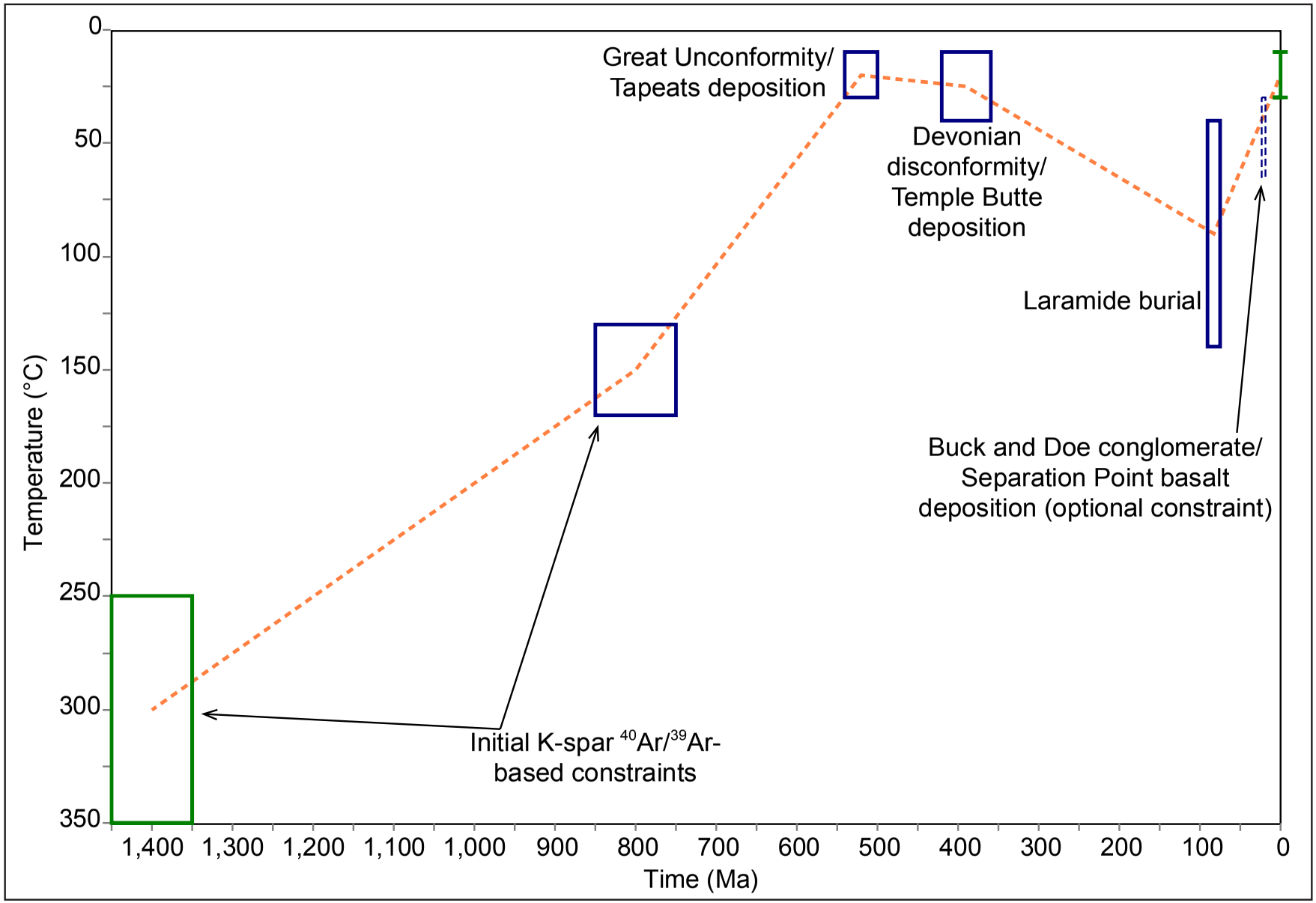

Figure 2. Constraint boxes imposed on the HeFTy modeling for all samples and their geologic justifications. The long period of time that samples resided in and below the partial retention zone between Precambrian and Laramide times may have resulted in extensive radiation damage to crystal lattices that was not fully annealed in the Laramide and hence produced complex and variable He diffusion behavior in apatite.

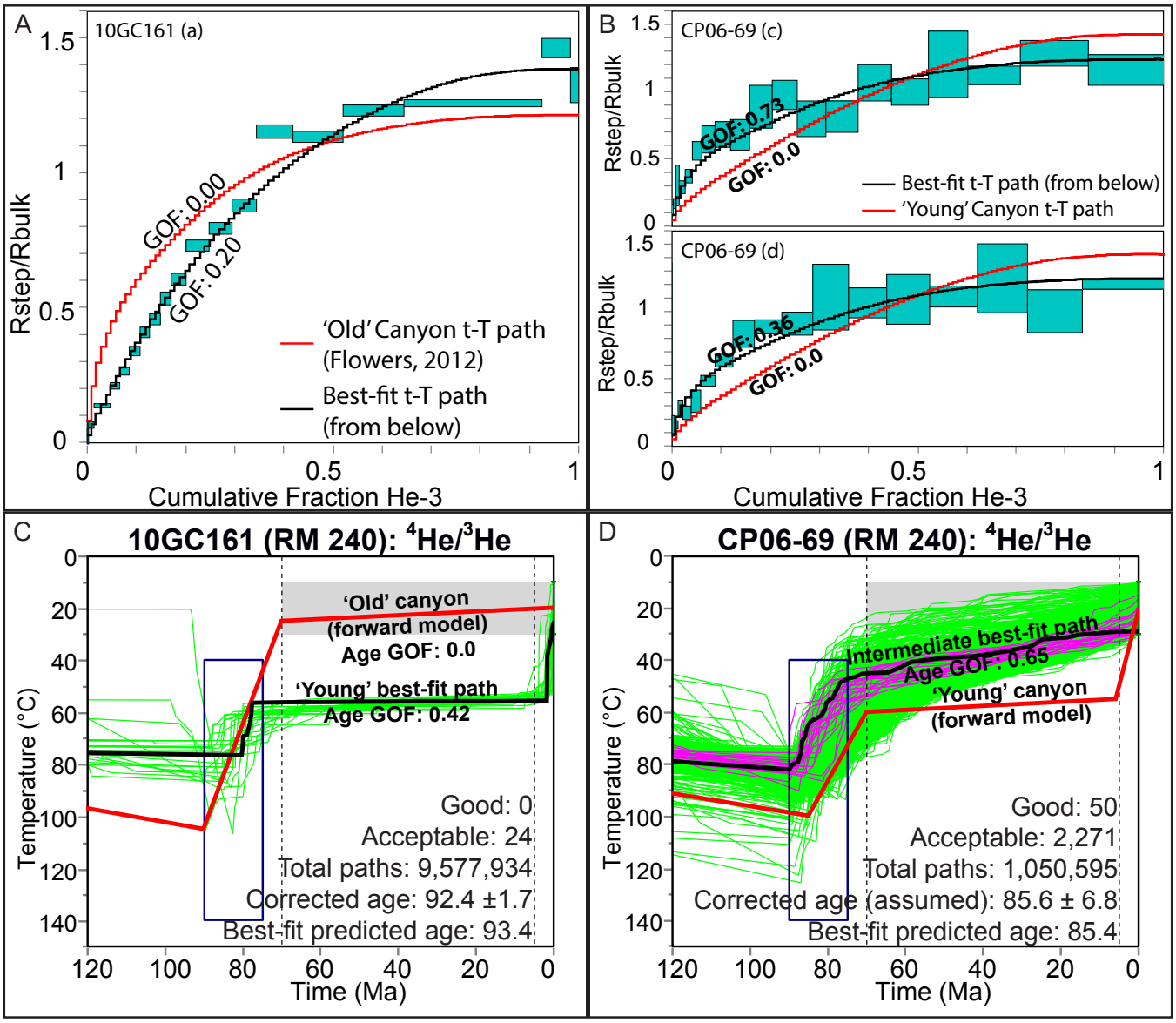

Figure 3. New and previously published $^{4}He/^{3}He$ data from 10GC161 and CP06-69, in the same location at Separation Canyon. A) New data are best predicted by the "young" canyon hypothesis. B) Flowers and Farley (2012) data are also best predicted by a "young" Canyon hypothesis. C) Inverse modeling of 10GC161-a using the measured age of this grain and assuming no zoning returned a tightly constrained "young" Canyon thermal history. D) Inverse modeling of the Flowers and Farley (2012) data using the same AHe age and error they used, which were not measured for this grain but were based on the mean AHe age and eU from other AHe analyses for this sample (Flowers et al., 2008). Note that good paths support a "young" canyon but reside at ~40 ˚C instead of 50-60 ˚C.

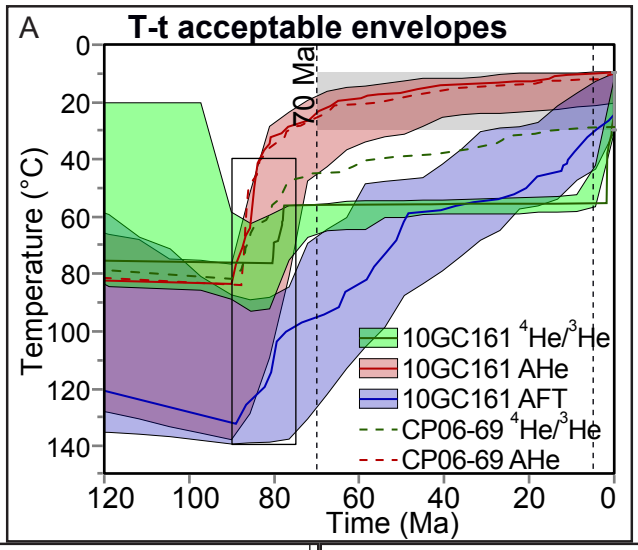

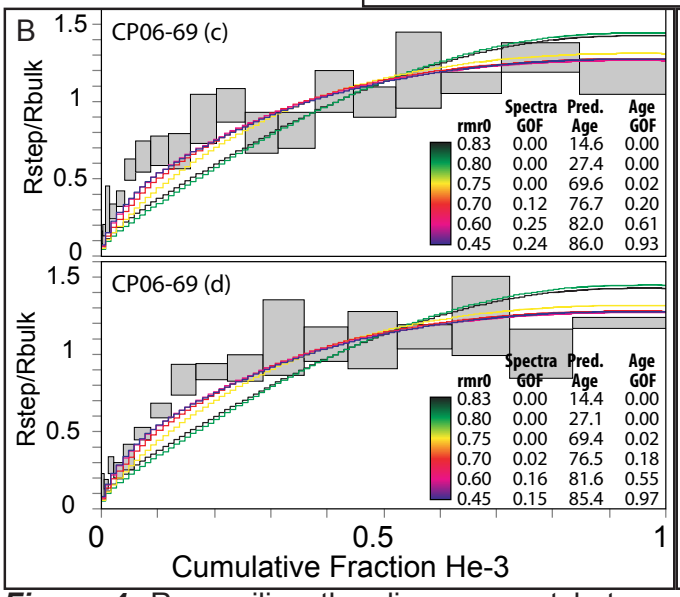

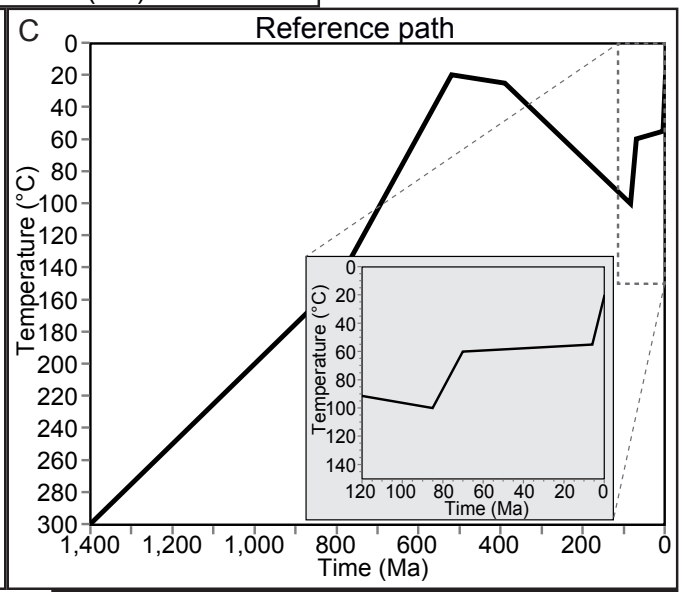

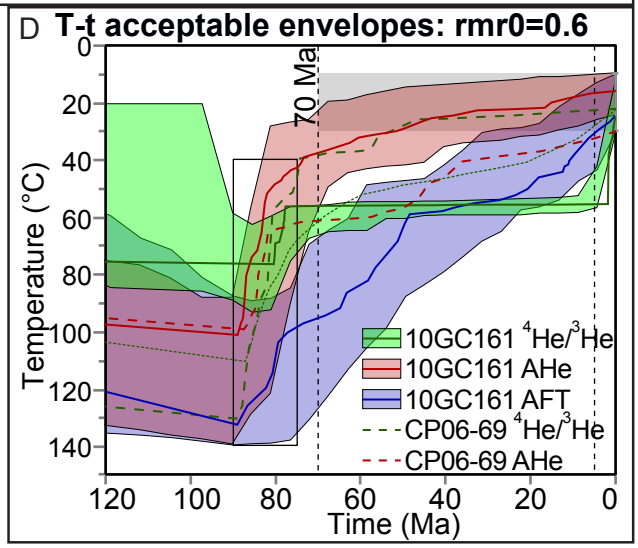

Figure 4. Reconciling the disagreement between Separation Canyon samples. A) t-T best-fit paths and envelopes from different samples (Sup. Fig. 1), all from the same locality at Separation Canyon, are geologically incompatible. B) To reconcile data, we adjust the rmr0 value (hence grain retentivity) in HeFTy for the Flowers and Farley (2012) samples to test the "young" canyon hypothesis and find that assuming higher grain retentivity (rmr0= 0.60) better predicts the $^{4}He/^{3}He$ data. C) Reference "young" Canyon t-T path for the predicted spectra in C. Inset shows a zoomed in area of the forward model after 120 Ma and above 150˚C, the time of interest for this study. D) t-T paths from all samples (and methods) from the Separation Canyon location can be brought into agreement with the "young" Canyon hypothesis (except the 10GC161 AHe t-T path) by using an assumed rmr0 of 0.60. Dotted line is the weighted mean path for $^{4}He/^{3}He$ data from CP06-69.

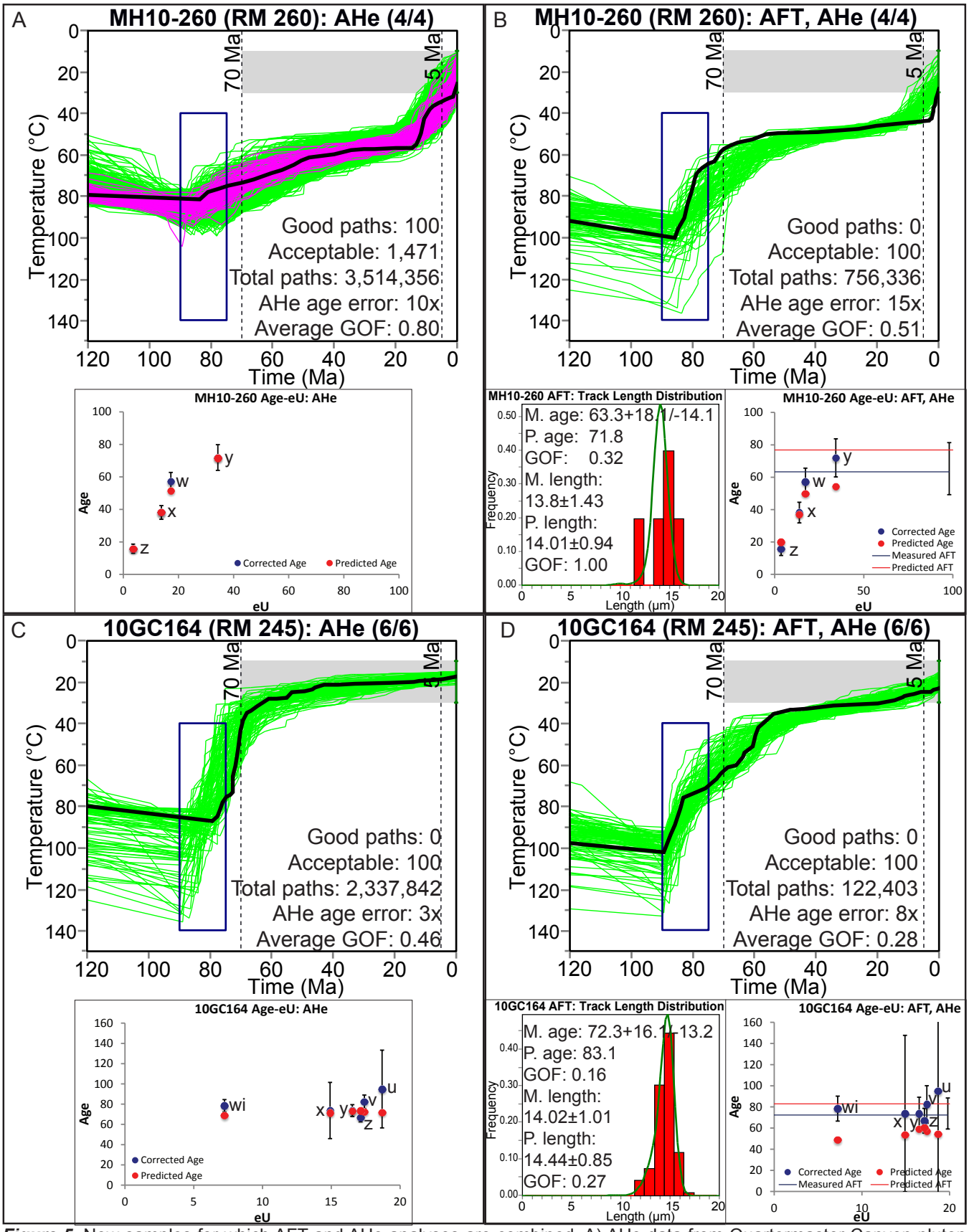

Figure 5. New samples for which AFT and AHe analyses are combined. A) AHe data from Quartermaster Canyon pluton (RM 260) are best predicted by a "young" Canyon t-T path. B) Combined AFT plus AHe data from the same samples predict a similar t-T path, but with higher Laramide peak T and cooler post-Laramide long-term residence T. C) AHe data from the 245-mile granodiorite are initially best predicted by an "old" Canyon t-T path. D) Combined modeling of AFT and AHe for the same sample as C are best predicted by a t-T path that resides at ~35 ºC from 60-20 Ma compatible with 0.4-1.0 km of burial depending on assumed surface T of 10-25 ºC (and geothermal gradient of 25 ºC/km).

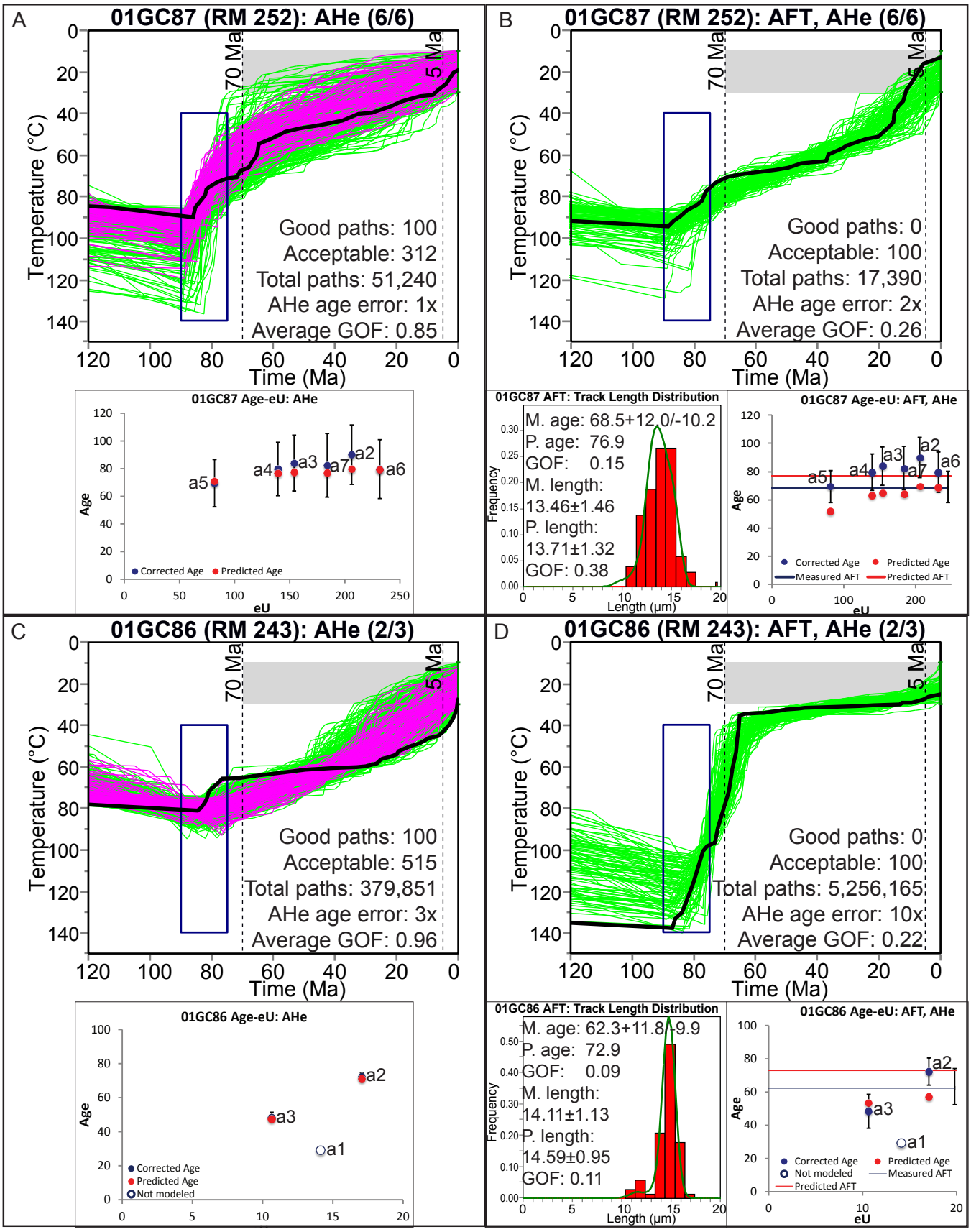

Figure 6. Previously published samples with combined AHe and AFT data. A) AHe data from the Surprise pluton are best predicted by a poorly constrained "young" Canyon t-T path. B) Combined AFT and AHe from the same sample as E are best predicted by a tightly constrained "young" Canyon t-T path. C) AHe data from the 245-mile granodiorite are best predicted by a "young" Canyon t-T path. D) Combined AHe and AFT data are best predicted by cooler post-Laramide residence but still a "young" Canyon path.

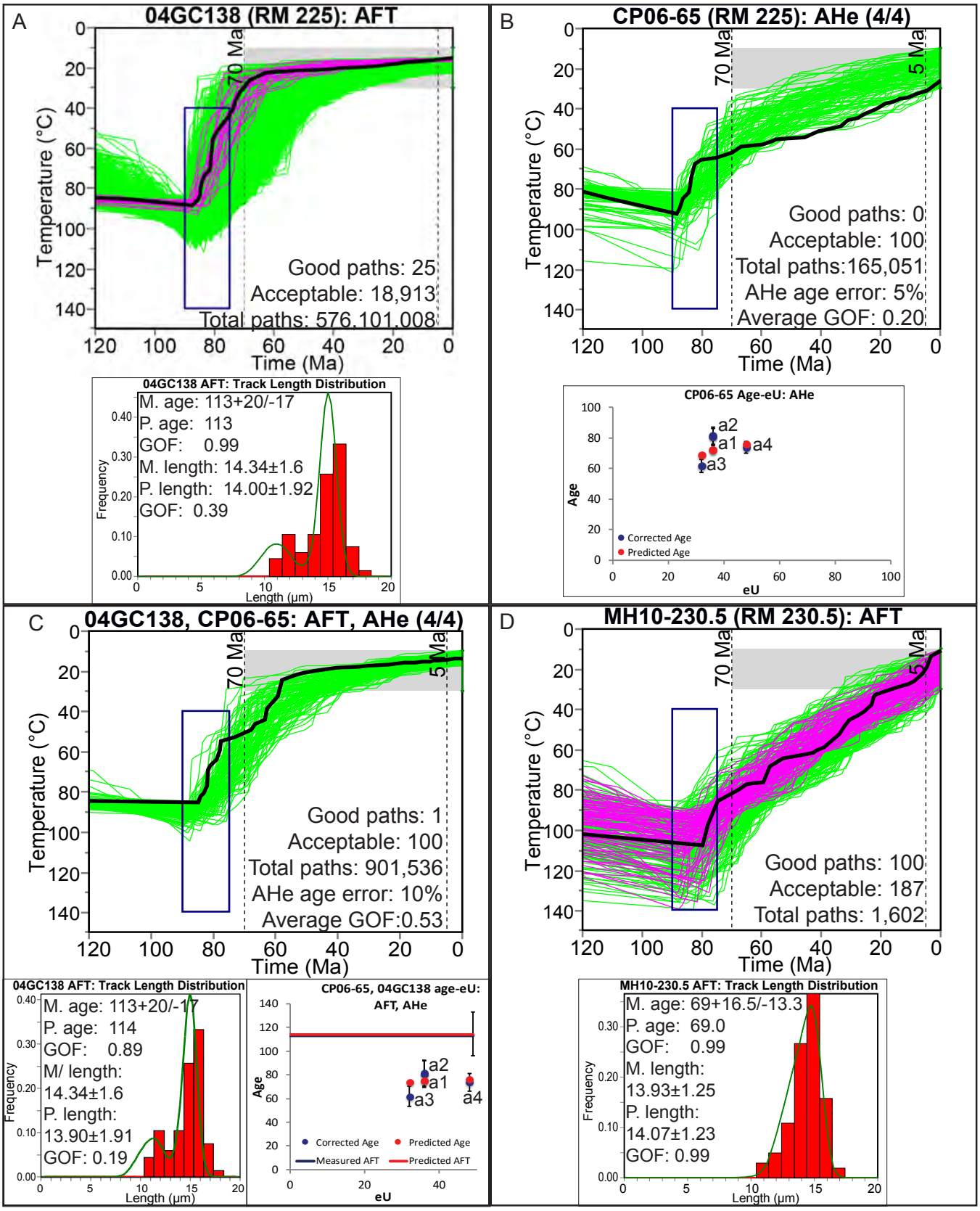

Figure 7: A "proof of concept" for samples from Diamond Creek would suggest that, because they are in the Hurricane segment, they should give "old" Canyon t-T paths (Karlstrom et al., 2014); A) New sample from the same location as a key sample from Kelley et al. (2001), where AFT data are best predicted by an "old" Canyon t-T path, consistent with this segment having been carved by the ~ 55-65 Ma Music Mountain Formation system. B) Previously published AHe data from Flowers (2008) that are best predicted by a "young" Canyon t-T path. C) Combined AFT and AHe data from A and B, respectively, are best predicted by t-T paths that reach surface temperatures by 60 Ma, compatible with the existence of a paleocanyon. D) New AFT data from river mile 230.5, best predicted by a "young" Canyon t-T path. Note the significant difference between this and A.

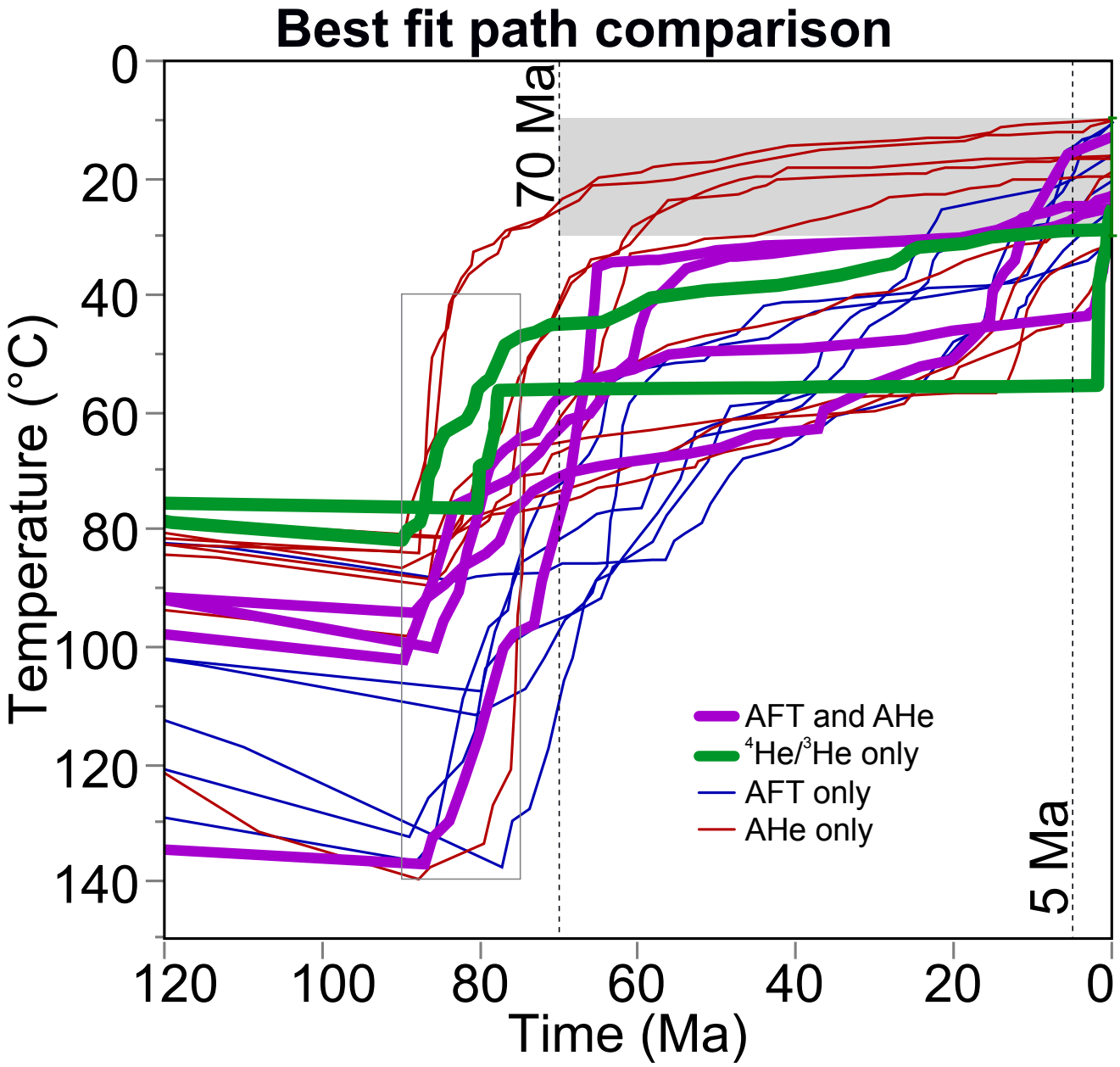

Figure 8. Best-fit path comparison for all samples shows inconsistent t-T paths. Our new $^{4}He/^{3}He$ data, the $^{4}He/^{3}He$ data from Flowers and Farley (2012), all combination models involving AFT and AHe, and about half the AHe-only analyses show post-Laramide residence time at 40-60 ºC from 70 to after 20 Ma, consistent with the "young" Canyon hypothesis. Five AHe-only best-fit paths are best predicted by t-T paths involving rapid cooling at 70 Ma, consistent with the "old" Canyon hypothesis (gray band). This range of t-T paths is not physically possible because many of the conflicting t-T paths are from the same location.

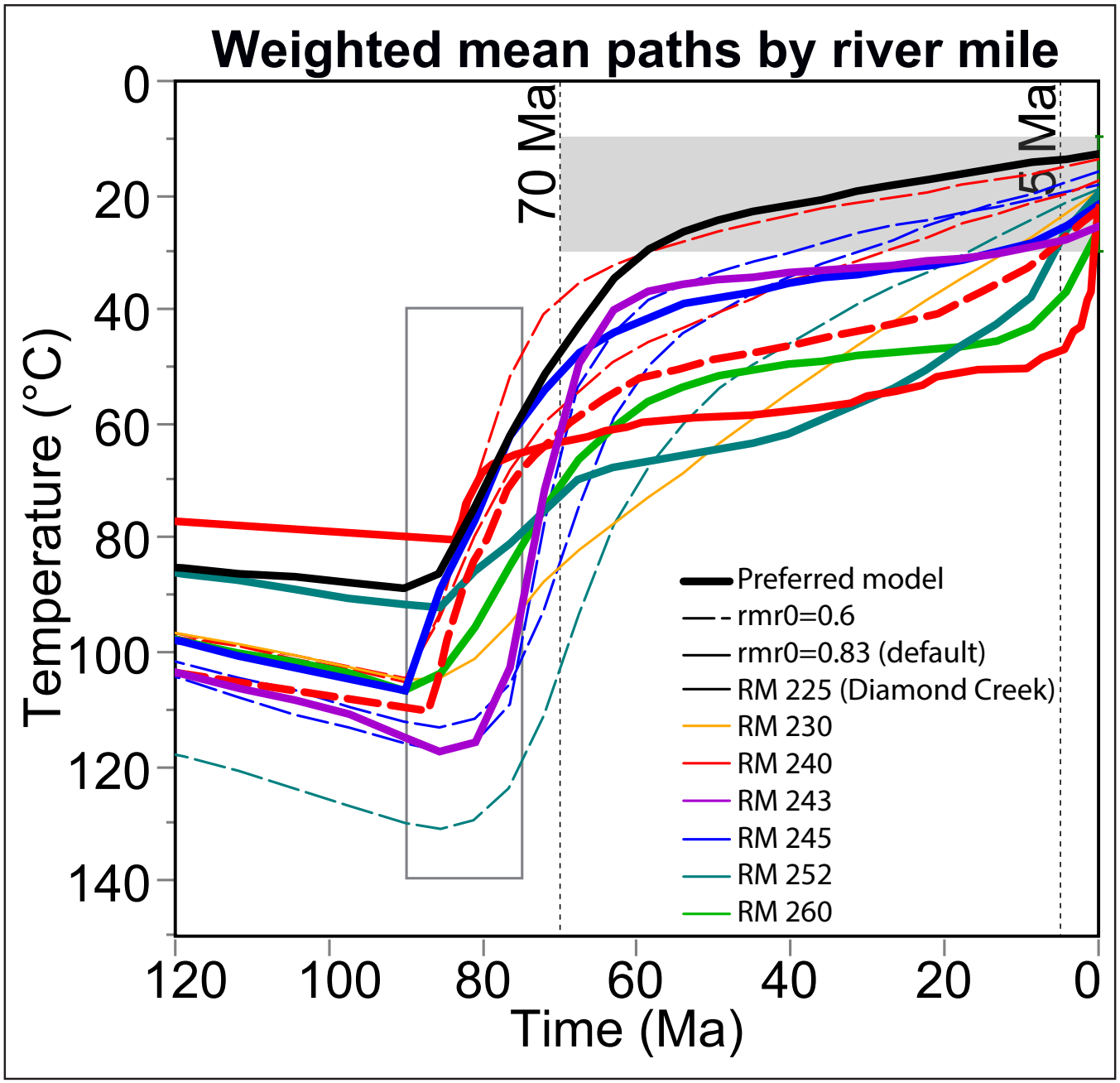

Figure 9. Synthesis of weighted mean t-T paths by river mile that shows preferred t-T paths based on the combination of multiple analytical techniques. The 'best' path for each sample was taken, including those with rmr0 values adjusted to 0.6 (dashed lines). Most t-T paths are more compatible with the "young" Canyon hypothesis, but post-Laramide residence T is varied. We have no good explanation for the AHe-only path at river mile 240 that is in conflict with AFT and $^{4}He/^{3}He$ best-fit paths even after setting rmr0 values to 0.6 (or even 0).

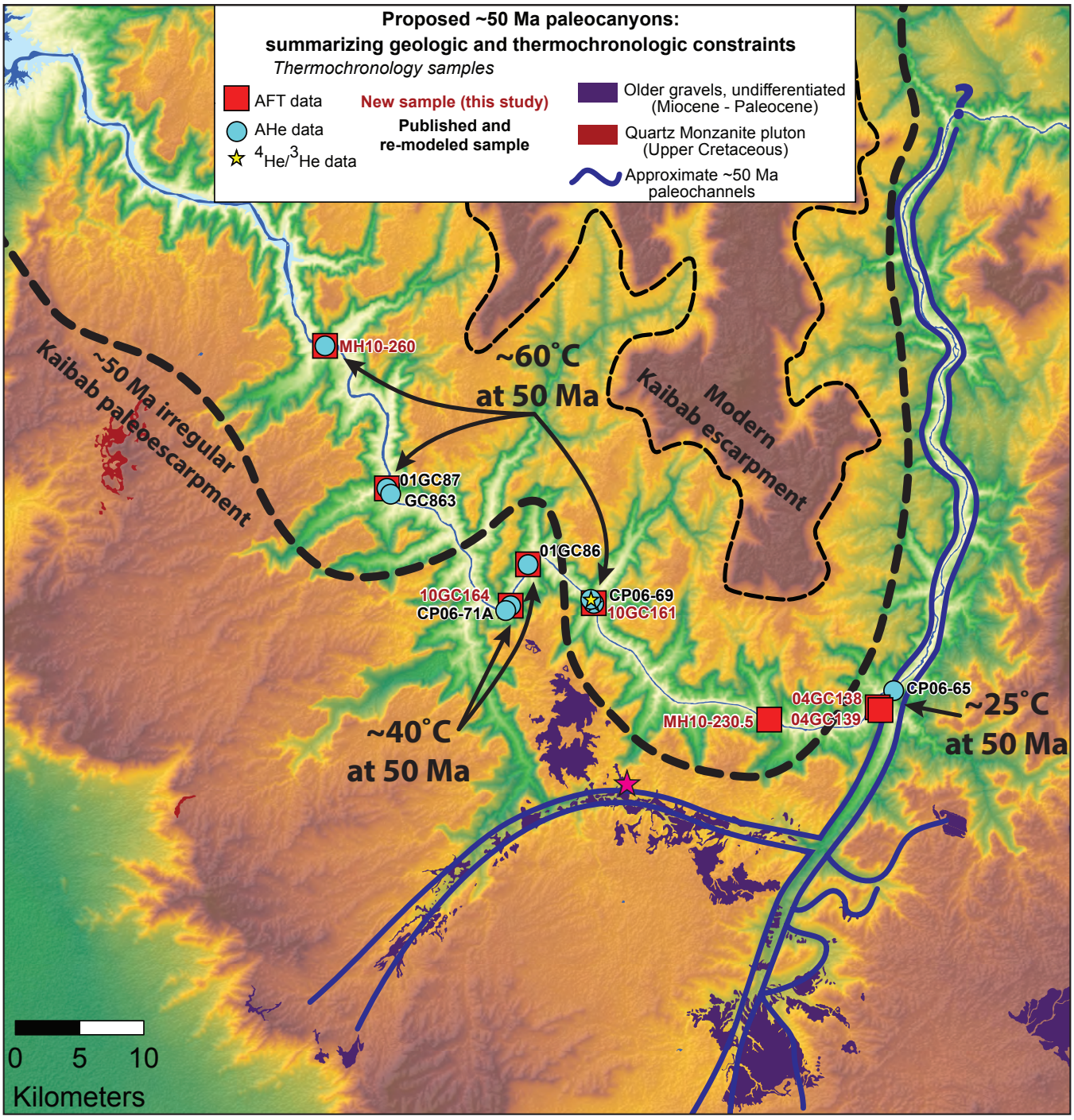

Figure 10. Summary figure showing irregular scarp retreat of the Kaibab escarpment. Paleorivers at Diamond Creek explain the cool temperatures of the combined AFT and AHe data there, while the extra 500m of material covering thermochronology samples at river mile 240, 252, and 260 explain the 10-20˚C higher temperatures observed in Figure 11 compared to samples located at river miles 243 and 245.